

1 **Kallikrein 13: a new player in coronaviral infections.**

2

3 Aleksandra Milewska^{1,2}, Katherine Falkowski², Magdalena Kalinska³, Ewa Bielecka³,
4 Antonina Naskalska¹, Pawel Mak⁴, Adam Lesner⁵, Marek Ochman⁶, Maciej Urlik⁶, Jan
5 Potempa^{2,7}, Tomasz Kantyka^{3,8}, Krzysztof Pyrc^{1,*}

6

7 ¹ Virogenetics Laboratory of Virology, Malopolska Centre of Biotechnology, Jagiellonian
8 University, Gronostajowa 7a, 30-387 Krakow, Poland.

9 ² Microbiology Department, Faculty of Biochemistry, Biophysics and Biotechnology,
10 Jagiellonian University, Gronostajowa 7, 30-387 Krakow, Poland.

11 ³ Laboratory of Proteolysis and Post-translational Modification of Proteins, Malopolska
12 Centre of Biotechnology, Jagiellonian University, Gronostajowa 7a, 30-387 Krakow,
13 Poland.

14 ⁴ Department of Analytical Biochemistry, Faculty of Biochemistry, Biophysics and
15 Biotechnology, Jagiellonian University, Gronostajowa 7 St., 30-387, Krakow, Poland.

16 ⁵ University of Gdansk, Faculty of Chemistry, Wita Stwosza 63, 80-308 Gdansk, Poland.

17 ⁶ Department of Cardiac, Vascular and Endovascular Surgery and Transplantology, Medical
18 University of Silesia in Katowice, Silesian Centre for Heart Diseases, Zabrze, Poland.

19 ⁷ Centre for Oral Health and Systemic Diseases, University of Louisville School of Dentistry,
20 Louisville, KY 40202, USA.

21 ⁸ Broegelmann Research Laboratory, Department of Clinical Science, University of Bergen,
22 5020 Bergen, Norway

23

24

25

26

27

28

29

30

31 * Correspondence should be addressed to **Krzysztof Pyrc** (k.a.pyrc@uj.edu.pl), Virogenetics

32 Laboratory of Virology, Malopolska Centre of Biotechnology, Jagiellonian University,

33 Gronostajowa 7, 30-387 Krakow, Poland; Phone number: +48 12 664 61 21; www:

34 <http://virogenetics.info/>.

35 **ABSTRACT**

36 Human coronavirus HKU1 (HCoV-HKU1) is associated with respiratory disease and is
37 prevalent worldwide, but *in vitro* model for virus replication is lacking. Interaction between the
38 coronaviral spike (S) protein and its receptor is the major determinant of virus tissue and host
39 specificity, but virus entry is a complex process requiring a concerted action of multiple cellular
40 elements. Here, we show that KLK13 is required for the infection of the human respiratory
41 epithelium and is sufficient to mediate the entry of HCoV-HKU1 to non-permissive RD cells.
42 We also demonstrated HCoV-HKU1 S protein cleavage by KLK13 in the S1/S2 region, proving
43 that KLK13 is the priming enzyme for this virus. Summarizing, we show for the first time that
44 protease distribution and specificity predetermines the tissue and cell specificity of the virus
45 and may also regulate interspecies transmission. It is also of importance that presented data may
46 be relevant for the emerging coronaviruses, including SARS-CoV-2 and may help to understand
47 the differences in their zoonotic potential.

48 **INTRODUCTION**

49 Coronaviruses are the largest group within the order *Nidovirales*. Mainly, they cause
50 respiratory and enteric diseases in humans and animals, but some can cause more serious
51 conditions such as hepatitis, peritonitis, or neurological disease. Seven coronaviruses infect
52 humans, four of which (human coronavirus [HCoV]-229E, HCoV-NL63, HCoV-OC43, and
53 HCoV-HKU1) cause relatively mild upper and lower respiratory tract disease and two (SARS-
54 CoV and MERS-CoV) are associated with severe, life-threatening respiratory infections and
55 multiorgan failure (1-6). Furthermore, in December 2019 a novel coronavirus SARS-CoV-2
56 emerged in Hubei province, China, causing pneumonia. To date, almost 90,000 cases were
57 identified and 3,000 patients died worldwide.

58 Coronaviral infection is initiated by interaction between the trimeric spike (S) protein
59 and its receptor, which is expressed on the surface of the susceptible cell. A number of adhesion
60 and entry receptors have been described for coronaviruses. For example, HCoV-229E (similar
61 to many other alphacoronaviruses) utilizes aminopeptidase N (APN) as the primary entry port
62 (7). Surprisingly, its cousin HCoV-NL63 shares receptor specificity with the evolutionarily
63 distant SARS-CoV and SARS-CoV-2: all hijack angiotensin-converting enzyme 2 (ACE2) (8-
64 11). HCoV-NL63 was also shown to use heparan sulfate as a primary attachment site (12-14).
65 A very different receptor is recognized by MERS-CoV, which binds to dipeptidyl-peptidase 4
66 (DPP4) (9, 15, 16). Another betacoronavirus, HCoV-OC43, binds to N-acetyl-9-O-
67 acetylneuraminic acid (17, 18). HCoV-HKU1 remains the great unknown because its cellular
68 receptor has not been identified and all efforts to culture the virus *in vitro* have failed.

69 HCoV-HKU1 was identified in Hong Kong in 2004. The virus was present in a sample
70 obtained from an elderly patient with severe pneumonia (19). Epidemiological studies show a
71 high prevalence of the pathogen in humans; this is because the majority of children seroconvert
72 before the age of 6 years (20, 21). While it is not possible to culture HCoV-HKU1 *in vitro*, we

73 and others reported that *ex vivo* fully differentiated human airway epithelium (HAE) and human
74 alveolar type II cells support the infection (22-25). A thorough study by Huang X *et al.*
75 demonstrated that HCoV-HKU1 binds to target cells *via* *O*-acetylated sialic acids on the cell
76 surface; however, this interaction is not sufficient for the infection. The study also showed that
77 the hemagglutinin-esterase (HE) protein of HCoV-HKU1 exhibits sialate-*O*-acetylsterase
78 activity and may act as a receptor-destroying enzyme, thereby facilitating the release of viral
79 progeny (26). Bakkers *et al.* proposed that, in order to adapt to the sialoglycome of the human
80 respiratory tract over the evolutionary timescale, HCoV-HKU1 lost the ability to bind to
81 attachment receptors *via* the HE protein (27). Recently, Hulswit *et al.* mapped the virus binding
82 site to *O*-acetylated sialic acids, demonstrating that the S1 domain A is responsible for binding
83 to the attachment receptor (28).

84 The S protein is the main player during coronavirus entry, and its characteristics
85 determine the host range. Coronaviral S proteins are class I fusion proteins comprising a large
86 N-terminal ectodomain, a hydrophobic trans-membrane region, and a small C-terminal
87 endodomain. The ectodomain is highly glycosylated and is composed of S1 and S2 domains.
88 The globular S1 domain is highly variable and carries the receptor-binding site, whereas the
89 more conserved rod-like S2 domain undergoes structural rearrangement during entry, which
90 brings the cellular and viral membranes into close proximity. Such a structural switch may be
91 triggered by different stimuli, including receptor binding, proteolytic cleavage of the S protein,
92 and/or a reduction in pH. Because different species require different stimuli, coronaviruses enter
93 cells at different subcellular sites. Some coronaviruses fuse at the plasma membrane, whereas
94 others are believed to enter the cell through receptor-mediated endocytosis, followed by fusion
95 deep within the endosomal compartments (29-35). Furthermore, recent reports show that the

96 entry portal may vary depending on tissue/cell characteristics. These differences may affect the
97 host range, pathogenicity, and cell/tissue specificity (1).

98 Host proteases prime coronaviral S proteins. For example, trypsin-mediated cleavage in
99 the small intestine is required for entry of porcine epidemic diarrhea virus (36), while a number
100 of coronaviruses from different genera (including HCoV-OC43, HCoV-HKU1, murine
101 hepatitis virus [MHV], MERS-CoV, and infectious bronchitis virus [IBV]) possess a furin
102 cleavage site (37-41). Kam *et al.* showed that SARS-CoV S protein can be cleaved by plasmin;
103 however, there is almost no biological evidence for its role *in vivo* (42). Cathepsins may also
104 act as S protein-activating enzymes. Indeed, cathepsin L processes the S proteins of SARS-
105 CoV, MERS-CoV, HCoV-229E, and MHV-2 (43-46). However, recent reports show that, *in*
106 *vivo*, respiratory coronaviruses may be activated by the TMPRSS2 protease, which enables
107 endocytosis-independent internalization, thereby re-shaping the entry process (45, 47-50).
108 While laboratory strains require priming by cathepsins, S proteins of clinical isolates (e.g.,
109 HCoV-229E and HCoV-OC43) undergo TMPRSS2-mediated cleavage at the cell surface,
110 which enables them to fuse with the cell membrane on the cell surface (51). A recent study by
111 Shirato *et al.* demonstrates that coronaviruses may lose their ability to infect naturally
112 permissive HAE cultures during cell culture adaptation because the S gene evolves and adjusts
113 to the proteolytic landscape of the immortalized cells (51).

114 Here, we identified a protease belonging to the tissue kallikrein (KLK) family as a new
115 player essential for HCoV-HKU1 entry to the target cell. The KLK family comprises 15 closely
116 related serine proteases with trypsin- or chymotrypsin-like specificity. The expression of these
117 enzymes is tightly regulated, and each tissue has its own unique KLK expression profile. These
118 enzymes play a role in a diverse range of processes during embryonic development to adulthood
119 (52-56), and some have been linked to human cancers (57-60). The function of some KLKs
120 remains to be elucidated, but obtained results suggest that protease distribution may be an

121 important factor pre-determining the cell and tissue specificity of the virus, but also regulating
122 the interspecies transfers.

123 Further, the data presented herein bring us a step closer to developing a convenient
124 *in vitro* culture model and possibly identifying the cellular receptor for this virus. It is also of
125 importance that presented data may be relevant for the emerging coronaviruses and may help
126 to understand the differences in their zoonotic potential.

127 **RESULTS**

128 **Several KLKs are upregulated after infection of HAE with HCoV-HKU1**

129 First, we asked whether HCoV-HKU1 infection modulates the expression of human
130 KLKs. HAE cultures were infected with HCoV-HKU1 or mock-inoculated. At 120 h post-
131 inoculation (p.i.), cells were collected and the expression of mRNAs encoding KLKs was
132 analyzed. We detected the expression of KLK7, KLK8, KLK10, KLK11, and KLK13 in
133 non-infected fully differentiated cultures. However, the pattern in HCoV-HKU1-infected cells
134 was different: we detected an upregulation of KLK7, KLK8, KLK10, KLK11 and KLK13.
135 Further, KLK1, KLK5, KLK6, KLK9, KLK12 and KLK14 were expressed in the infected cells.
136 KLK2, KLK3, and KLK15 were not expressed (**Fig. 1**).

137

138 **KLK13 is essential for HCoV-HKU1 infection**

139 S protein priming is a prerequisite for coronavirus entry; therefore, we tested whether
140 KLKs take part in this process by culturing cells in the presence/absence of KLK inhibitors (
141 **Table 1**) (61). For this, HAE cultures were pre-incubated with each inhibitor (10 μ M) or with
142 vehicle control (DMSO) and mock-inoculated or inoculated with the virus (10⁶ RNA copies per
143 ml) in the presence of the inhibitor. Apical washes were collected each day for analysis of virus
144 replication. Subsequently, viral RNA was isolated and reverse transcribed (RT), and the HCoV-
145 HKU1 yield was determined by quantitative real-time PCR (qPCR). The results showed that
146 HCoV-HKU1 replication was inhibited in the presence of a KLK13 inhibitor; this was not the
147 case for cells treated with DMSO or with inhibitors specific for KLK7 or KLK8 (**Fig. 2A**).

148 Next, we analyzed HCoV-HKU1 replication in the presence of a family-specific KLK
149 inhibitor SPINK6 at a concentration of 10 μ g/ml (62, 63) or 100 μ M camostat (a broad inhibitor
150 of serine proteases, also a potent inhibitor of KLK13) (34, 64). We noted inhibition of

151 HCoV-HKU1 replication in the presence of both inhibitors (**Fig. 2B**). All inhibitors were used
152 at non-toxic concentrations (**Fig. 2C**).

153 The experiments conducted so far suggested that KLK13 is required for virus infection.
154 However, one may question the specificity of the KLK13 protease inhibitors. To ensure that
155 KLK13 is indeed the priming enzyme during HCoV-HKU1 infection, we developed HAE
156 cultures by transforming cells with lentiviral vectors encoding shRNAs targeting KLK13
157 mRNA. We then confirmed that the expression of the protease was silenced (HAE_shKLK13).
158 Non-modified HAE cultures (HAE_ctrl), cultures modified using a lentiviral vector to express
159 the GFP protein (HAE_GFP), and HAE cultures transduced with an empty lentiviral vector
160 (HAE_vector) were used as controls. Following transduction and differentiation, expression of
161 KLK13 mRNA in HAE_shKLK13 was almost undetectable, in contrast to the control cultures
162 (**Fig. 3A**). Importantly, HAE_shKLK13 cells continued to differentiate and formed
163 pseudostratified cultures (**Fig. 3B**). Next, we infected HAE_ctrl, HAE_GFP, HAE_vector, and
164 HAE_shKLK13 with HCoV-HKU1 (10^6 RNA copies per ml) and incubated them for 2 h at
165 32°C with the viral stock solution. Cultures were maintained at 32°C for 5 days at an air-liquid
166 interface. Apical washes were collected, and virus yield was determined by RT-qPCR. We
167 found that, in contrast to that in control cultures, replication of virus in HAE_shKLK13 was
168 abolished (**Fig. 3C**). Overall, these data suggest that silencing the *KLK13* gene in HAE inhibits
169 virus infection, indicating that KLK13 is necessary for HCoV-HKU1 infection.

170

171 **KLK13 enables entry of HCoV-HKU1 pseudoviruses**

172 We determined that KLK13 is essential for efficient HCoV-HKU1 infection in HAE
173 cultures and we started to wonder whether this enzyme may be a determinant of the cell and
174 tissue specificity of the virus. Previous studies showed that RD cells support virus attachment
175 *via* sialic acids, but this does not allow for the virus entry (26). To test whether cell surface

176 proteases my render RD cells permissive, we generated RD cells expressing human KLK13 or
177 TMPRSS2 proteases. RD cells were transduced with lentiviral vectors harboring the KLK13
178 gene (RD_KLK13), control vector (RD_ctrl), or TMPRSS2 (RD_TMPRSS2). Due to the lack
179 of KLK13 specific antibodies, we verified its presence based on RT-PCR (**Fig. 4A**). The
180 presence of TMPRSS2 in RD_TMPRSS2 cells was confirmed using Western blot. The
181 TMPRSS2 band in RD cells was observed at 25 kDa, which corresponds to one of the naturally
182 occurring splicing variants (**Fig. 4B**). Subsequently, we transduced RD_ctrl, RD_KLK13 and
183 RD_TMPRSS2 cells with HIV particles pseudotyped with HCoV-HKU1 S glycoprotein
184 (S-HKU1), control VSV G protein (VSV-G) or lacking the fusion protein (Δ Env). After 3 day
185 culture at 37°C, pseudovirus entry was quantified by measurement of the luciferase activity. As
186 shown in **Fig. 4C**, all cultures were effectively transduced with control VSV-G vectors, while
187 only RD_KLK13 cells were permissive to S-HKU1 pseudoviruses. This clearly showed that
188 KLK13, and not TMPRSS2 is involved in HCoV-HKU1 entry. Furthermore, S-HKU1, d VSV-
189 G and Δ Env pseudoviruses were overlaid onto fully differentiated HAE cultures in the presence
190 of KLK13 inhibitor (10 μ M) or DMSO. After 3 day culture at 37°C pseudovirus entry was
191 quantified by measurement of the luciferase activity. Despite low transduction efficiency in
192 HAE, we observed an increase in luciferase activity in cultures treated with S-HKU1
193 pseudoviruses, compared to Δ Env, which was completely abolished in the presence of KLK13
194 inhibitor (**Fig 4D**). Overall, these data demonstrated that KLK13 activity drives HCoV-HKU1
195 entry into cells.

196

197 **KLK13 enables the replication of HCoV-HKU1 in RD cells**

198 Obtained results showed that KLK13 expression on RD cells was sufficient for HCoV-
199 HKU1 pseudovirus entry. Here, we aimed to test whether KLK13 presence renders RD cells
200 permissive for HCoV-HKU1 infection. For this, we infected RD_ctrl and RD_KLK13 cells

201 with HCoV-HKU1 (10^8 RNA copies per ml) and incubated the culture for 7 days at 32°C in the
202 presence or absence of a KLK13 inhibitor ($10\ \mu\text{M}$) or DMSO. Next, cellular RNA was isolated
203 and the presence of HCoV-HKU1 N subgenomic mRNA (N sg mRNA), which is considered
204 to be a hallmark of coronaviral infection, was assessed (14). sg mRNA appeared in RD_KLK13
205 cells, while no signal was detected in cultures supplemented with the KLK13 inhibitor nor in
206 RD_ctrl cells (**Fig. 5A**).

207 To further confirm the role of KLK13 during HCoV-HKU1 infection RD cells were
208 supplemented with purified human KLK13 or KLK14 (61). The latter was used as a negative
209 control. Virus stock was incubated for 2 h at 32°C with 200 nM KLK13, KLK14, or trypsin or
210 control (PBS). Next, RD cells were incubated for 7 days at 32°C with the virus (diluted 10-fold
211 in DMEM) or mock samples (in DMEM), after which cellular RNA was isolated and
212 HCoV-HKU1 infection was analyzed by means of N sg mRNA detection. Again, we found that
213 N sg mRNA was produced only in the presence of KLK13 (**Fig. 5B**). Further, we passaged
214 HCoV-HKU1 twice in RD cells. Briefly, 1 ml of cell culture supernatant from the first
215 experiment was transferred to fresh RD cells and fresh enzymes were added (final concentration
216 200 nM). Cultures were then incubated at 32°C for 7 days. Cellular RNA was isolated and
217 HCoV-HKU1 infection was monitored by detecting N sg mRNA. The infection occurred only
218 in the presence of KLK13 (**Fig. 5B**). However, we observed no cytopathic effects (CPEs), and
219 replication levels were very low (no significant increase over control levels on RT-qPCR; data
220 not shown). To further test the effect of KLK13 on replication of HCoV-HKU1 in RD cells, the
221 virus stock was incubated with purified KLK13 (200 nM) and incubated in the presence or
222 absence of a KLK13 inhibitor ($10\ \mu\text{M}$) or DMSO. After 2 h at 32°C pre-treated virus stock was
223 diluted in media as described above and overlaid on RD cells. After 7 days at 32°C we evaluated
224 the presence of the HCoV-HKU1 N sg mRNA. The virus replicated only after treatment with
225 KLK13, and supplementation with the inhibitor blocked this effect infection (**Fig. 5C**).

226

227 **KLK13 primes the HCoV-HKU1 S protein**

228 Expression of KLK13 by cells previously resistant to HCoV-HKU1 renders them
229 susceptible; therefore, we asked whether this is due to proteolytic activation of the S protein.
230 We tested this using the CleavEx method, in which a peptide of interest is exposed in the
231 N-terminal region of the proteolytically-resistant HmuY carrier protein. Briefly, two-hybrid
232 His-tagged CleavEx proteins were prepared, both harboring 8-amino acid peptide sequences of
233 the HCoV-HKU1 S protein. The first peptide contained the S1/S2 cleavage site (amino acids
234 757–764), which in some coronaviruses is activated during protein biosynthesis, during virus
235 exocytosis, or after receptor engagement. The second harbored the S2/S2' cleavage site (amino
236 acids 901–908), which is an additional region prone to proteolytic cleavage (25, 38). Proteins
237 were purified and further incubated for 3 h at 37°C with increasing concentrations of purified
238 KLK13. Subsequently, proteins were resolved by SDS-PAGE and detected by western blotting
239 with antibodies specific for His-tagged proteins. The analysis showed that, in the presence of
240 500 nM KLK13, the CleavEx protein harboring the S1/S2 cleavage site was degraded; however,
241 the CleavEx protein harboring the S2/S2' site remained intact. Because KLKs are produced as
242 pro-forms that undergo self-activation, an additional band of His-tagged purified pro-KLK13
243 (HisTag-pro-KLK13) was observed after treatment with 500 nM KLK13 (**Fig. 6A**). The product
244 of the S1/S2 cleavage was further sequenced by N-terminal Edman degradation showing the
245 following sequence: R↓SISA, which corresponds to the S1/S2 site. This result shows clearly
246 that the S1/S2 region of the HCoV-HKU1 S protein is prone to KLK13-mediated cleavage.

247 Furthermore, we aimed to confirm the cleavage using a full-length Spike protein of
248 HCoV-HKU1 (HKU1-S). For this, we expressed the HKU1-S in 293T cells, purified the protein
249 using 6 × His tag, and incubated for 3 h at 37°C with increasing concentrations of purified
250 KLK13. Subsequently, HKU-S or mock proteins were resolved by SDS-PAGE and detected by

251 western blotting with antibodies specific to the tag. The analysis showed that in the presence of
252 1 μ M KLK13 the HKU1-S was degraded (**Figure 6B**). The S protein was observed at
253 ~150 kDa, which is consistent with the migration speed reported for these highly glycosylated
254 proteins (*I*).
255

256 **DISCUSSION**

257 Receptor recognition is the first, essential step of the virus infection process. The
258 coronaviral S protein mediates virus entry into host cells by binding to a specific receptor. A
259 combination of stimuli, e.g., receptor binding, proteolytic cleavage, and exposure to low pH
260 results in rearrangement of the S protein and, consequently, to membrane fusion and virus entry
261 (*1*). Although the structure of both the HCoV-HKU1 S ectodomain and the receptor-binding
262 domain has been resolved, the receptor determinant remains unknown (28, 38, 65). In a previous
263 study, we showed that HCoV-HKU1 utilizes *O*-acetylated sialic acids on host cells as an
264 attachment receptor (26). Here, we present data demonstrating that the protease KLK13 is
265 required for HCoV-HKU1 infection of the respiratory epithelium.

266 Human KLKs take part in multiple physiological processes, including skin
267 desquamation, tooth enamel formation, kidney and brain function, and synaptic neural plasticity
268 (66-75). Also, recent studies demonstrate a role for some KLKs during viral infections. For
269 instance, KLK8 plays a role in the proteolytic activation of the human papillomavirus capsid
270 protein, thereby mediating virus entry into host cells (76). Also, KLK5 and KLK12 are secreted
271 into the respiratory tract, where they support replication of the influenza A virus by cleaving
272 the hemagglutinin protein (77, 78); however, these proteins belong to a large pool of cell surface
273 proteases, the orchestrated action of which promotes virus replication.

274 Here, we found that the yield of HCoV-HKU1 from HAE fell in the presence of SPINK6
275 (inhibitor of KLK13) (62, 63) and camostat (a broad range inhibitor of serine proteases).
276 However, the first compound also inhibits other KLKs (63), while the second block the activity
277 of a wide range of serine proteases and was used previously to demonstrate the role of
278 TMPRSS2/4 proteases during viral infection (34, 45, 51, 64, 79, 80). The relatively low
279 inhibition of HCoV-HKU1 replication in the presence of SPINK6 possibly results from non-
280 optimal compound concentration at the HAE cultures, and cytotoxicity at higher

281 concentrations(63). Broad spectrum protease inhibitors are now used widely for virus research,
282 although their non-specific activity makes the results equivocal. For example, Matsuyama *et al.*
283 showed recently that the furin inhibitor dec-RVKR-CMK interferes with the activity of several
284 proteases, and that its previously described inhibitory activity during MERS-CoV infection is
285 not specific to furin; instead, its activity is due to non-specific inhibition of cathepsin L and
286 TMPRSS2 (81). We tried to use specific KLK inhibitors developed in our laboratory (61).
287 Considering the small arsenal of tools available to researchers studying KLKs, only three
288 compounds were readily available. Treating HAE cultures with these inhibitors revealed that
289 only compounds designed to inhibit KLK13 hampered HCoV-HKU1 replication. However, the
290 great similarity between different KLKs makes one doubt the specificity of these inhibitors,
291 despite their performance in biochemical assays. Therefore, we decided to silence KLK13 in
292 HAE cultures. This abolished virus replication *ex vivo*, thereby confirming the importance of
293 KLK13 during infection. KLK13 is thought to be secreted and membrane-bound(82, 83).

294 This study showed that HCoV-HKU1 infection in HAE modulates the expression of
295 different KLKs, including KLK13. In our study, KLKs expression was tested using semi-
296 quantitative PCR, and for that reason, we were unable to show the level of KLKs modulation
297 after HCoV-HKU1. However, the pattern of virus-induced expression of several KLKs could
298 be observed. KLK mechanism of activation is a complex process and until now it has only
299 been proven that most KLK genes are regulated by steroids and other hormones (84). It is also
300 important to remember, that KLK expression is regulated in a similar manner, and the induction
301 of a single gene usually results in overexpression of the whole cluster (85, 86). While one may
302 assume that the virus stimulates KLK13 production to promote the infection, this up-regulation
303 is likely a natural response of the damaged tissue, as KLKs were previously reported to take
304 part also in tissue regeneration (87-89). Further, increased expression of KLKs may be the

305 response to the inflammatory process, as Seliga *et al* demonstrated that KLK-kinin system is a
306 potent modulator of innate immune responses (90).

307 The experiments performed herein show the importance of KLK13 for virus entry into
308 susceptible cells; therefore, we speculated that scattered distribution of different KLKs in
309 different tissues may be one of the determinants of the HCoV-HKU1 tropism (53, 91). We
310 tested the purified enzyme expressed in the eukaryotic cells; however, we also developed a cell
311 line constitutively expressing the enzyme. As an *in vitro* model for our studies, we used RD
312 cells previously reported to carry attachment receptors for the virus (26). Here, using
313 pseudoviruses decorated with S-HKU1 proteins we showed that KLK13 presence on RD cells
314 is sufficient for virus entry and renders these cells permissive. Our experiments also showed
315 that in contrast to previous reports, TMPRSS2 is not involved in this process(51). Furthermore,
316 we observed that RD cells supported the replication of the virus in the presence of KLK13 and
317 that this effect was reversed in the presence of the specific KLK13 inhibitor. We were, however,
318 not able to culture the virus to high yields. HCoV-HKU1 replication in KLK13-expressing RD
319 cells remained inefficient and RTqPCR assessment did not reveal significant increases in the
320 amounts of viral RNA. For that reason, we are only able to detect viral sg mRNAs, which are
321 considered to be the hallmark of coronaviral replication. We believe that this may be due to
322 non-optimal infection conditions, which may include inappropriate KLK13 concentrations or
323 low density of the entry receptor. Also, it is possible that RD cells may not support efficient
324 replication of the virus due to factors unrelated to the entry process. Nonetheless, our results
325 show that the HCoV-HKU1 entry receptor is present on RD cells, and we were able to trigger
326 virus entry and replication; these findings warrant further exploration.

327 Most coronaviral S proteins are processed into S1 and S2 subunits by host proteases,
328 which allows conformational changes in the S protein and leads to fusion of the viral and
329 cellular membranes (1, 92). As shown in the recent work by Kirchdoerfer *et al.*, the

330 HCoV-HKU1 S protein has two regions that are prone to proteolytic activation: the S1/S2 furin
331 cleavage site and a secondary cleavage site termed S2', which is adjacent to a potential fusion
332 peptide (38). While the S1/S2 site is believed to be processed by furin during protein
333 biosynthesis, the S2/S2' site is expected to be cleaved during virus entry. As we already knew
334 that KLK13 is sufficient for HCoV-HKU1 infection of naturally non-permissive RD cells, we
335 aimed to investigate whether this was the direct result of KLK13-mediated proteolytic cleavage
336 of the S protein. For this, we employed the CleavEx method, in which peptide of interest is
337 coupled to the carrier HmuY protein and then undergoes proteolytic cleavage by the enzyme
338 being tested. We found that the S1/S2 site was efficiently cleaved by KLK13, whereas the
339 S2/S2' region remained intact. As CleavEx technique is a convenient surrogate system allowing
340 for precise mapping of the cleavage site, it has some limitations. To ensure the reliability of
341 results, purified full-length HCoV-HKU1 S protein was subjected to the proteolytic cleavage.
342 Also here we observed efficient cleavage of the HCoV-HKU1 S protein by KLK13.

343 While the results presented here show that KLK13 is able to process the HCoV-HKU1
344 S protein, one may question whether the cleavage is sufficient for HCoV-HKU1 entry. It was
345 previously presented for MERS-CoV that two consecutive enzymatic scissions are required for
346 activation of the S protein. In this scenario, KLK13 would prime the HCoV-HKU1 S at S1-S2
347 site, enabling scission at S2-S2' site by the TMPRSS2 or another host protease (38, 40, 93).
348 This may be one of the factors limiting the HCoV-HKU1 replication in RD_KLK13 cells, as
349 only minimal replication is observable.

350 Summarizing, we show that KLK13 is a key determinant of HCoV-HKU1 tropism. This
351 may explain why, since its first identification in 2004, all efforts to culture HCoV-HKU1 in
352 standard cell lines have failed. We believe that this study increases our knowledge of HCoV-
353 HKU1 and may promote the future in-depth investigation of coronaviruses. Considering the
354 increasing number and diversity of coronaviruses, and the proven propensity of coronaviruses

355 to cross the species barrier and cause severe diseases in humans, further research on the role of
356 different proteases in coronaviral infections is necessary.

357 MATERIALS AND METHODS

358 Plasmid constructs

359 KLK13 and TMPRSS2 genes were amplified by PCR using cDNA obtained from HAE
360 cells. Each PCR product was cloned into pWPI plasmid for lentivirus production and sequence
361 verified. pLKO.1-TRC cloning vector was a gift from David Root (Addgene plasmid #
362 10878)(94). Oligonucleotides for the generation of shRNA against KLK13 (3 different shRNAs
363 targeting the exons encoding the active site) were hybridized and cloned into pLKO.1-TRC
364 vector. The full-length HKU1-S gene was amplified by PCR using pCAGGS/HKU1-S plasmid
365 that was a gift from Xingchuan Huang. The PCR product was cloned into pSecTag2 cloning
366 vector and sequence verified. Primer sequences are provided in **Table 2**.

367

368 Cell culture

369 RD (*Homo sapiens* muscle rhabdomyosarcoma; ATCC: CCL-135) and 293T (*Homo*
370 *sapiens* kidney epithelial; ATCC: CRL-3216) cells were cultured in Dulbecco's MEM (Thermo
371 Fisher Scientific, Poland) supplemented with 3% fetal bovine serum (heat-inactivated; Thermo
372 Fisher Scientific, Poland) and antibiotics: penicillin (100 U/ml), streptomycin (100 µg/ml), and
373 ciprofloxacin (5 µg/ml). Cells were maintained at 37°C under 5% CO₂.

374

375 Human airway epithelium (HAE) cultures

376 Human epithelial cells were isolated from conductive airways resected from transplant
377 patients. The study was approved by the Bioethical Committee of the Medical University of
378 Silesia in Katowice, Poland (approval no: KNW/0022/KB1/17/10 dated 16.02.2010). Written
379 consent was obtained from all patients. Cells were dislodged by protease treatment, and later
380 mechanically detached from the connective tissue. Resulting primary cells were first cultured
381 in the selective media to proliferate in the presence of the Rho-associated protein kinase

382 (ROCK) inhibitor (Y-27632, 10 $\mu\text{g/ml}$, Sigma-Aldrich, Poland) (95). Further, cells were
383 trypsinized and transferred onto permeable Transwell insert supports ($\phi = 6.5$ mm). Cell
384 differentiation was stimulated by the media additives and removal of media from the apical side
385 after the cells reached confluence. Cells were cultured for 4-6 weeks to form well-differentiated,
386 pseudostratified mucociliary epithelium (96). All experiments were performed in accordance
387 with relevant guidelines and regulations.

388

389 **Cell viability assay**

390 HAE cultures were prepared as described above. Cell viability assay was performed by
391 using the XTT Cell Viability Assay (Biological Industries, Israel), according to the
392 manufacturer's instructions. Briefly, on the day of the assay 100 μl of the $1 \times$ PBS with the
393 30 μl of the activated XTT solution was added to each well/culture insert. Following 2 h
394 incubation at 37°C , the solution was transferred onto a 96-well plate and the signal was
395 measured at $\lambda = 490$ nm using the colorimeter (Spectra MAX 250, Molecular Devices). The
396 obtained results were further normalized to the control sample, where cell viability was set to
397 100%.

398

399 **Virus infection**

400 HAE cultures were washed thrice with 100 μl of $1 \times$ PBS, following inoculation with
401 HCoV-HKU1 (strain Caen 1) or mock (cell lysate). After 2 h incubation at 32°C unbound
402 virions were removed by washing with 100 μl of $1 \times$ PBS and HAE cultures were cultured at
403 air-liquid interphase until the end of the experiment. Due to the lack of a permissive cell line it
404 was not possible to titrate the virus stock for infection experiments and therefore the inoculum
405 was quantified using RT-qPCR.

406 RD cells grown in 90% confluency were infected with HCoV-HKU1 (10^8 RNA copies per
407 ml) in Dulbecco's MEM (Thermo Fisher Scientific, Poland) supplemented with 3% fetal bovine
408 serum (heat-inactivated; Thermo Fisher Scientific, Poland) and antibiotics: penicillin
409 (100 U/ml), streptomycin (100 μ g/ml). Cells were incubated for seven days at 32°C, washed
410 thrice with $1 \times$ PBS, and collected for RNA isolation in Fenzol reagent (A&A Biotechnology,
411 Poland). All research involving the infectious material was carried out adhering to the biosafety
412 regulations. All research involving genetic modifications was carried out adhering to the
413 national and international regulations.

414

415 **Lentivirus production and transduction**

416 293T cells were seeded on 10 cm² dishes, cultured for 24 h at 37°C with 5% CO₂ and
417 transfected with psPAX, pMD2G and third transfer plasmid (pWPI/KLK13, pLKO.1-
418 TRC/shrnaKLK13 or Lego-G2) using polyethyleneimine (Sigma-Aldrich, Poland). psPAX
419 (Addgene plasmid # 12260) and pMD2G (Addgene plasmid # 12259) was a gift from Didier
420 Trono. pLKO.1 - TRC cloning vector was a gift from David Root (Addgene plasmid # 10878)
421 (94). Cells were further cultured for 96 h at 37°C with 5% CO₂ and lentiviral particles were
422 collected every 24 h and stored at 4°C. Lentivirus stocks were concentrated 25-fold using
423 centrifugal protein concentrators (Amicon Ultra, 10-kDa cutoff; Merck, Poland) and stored at -
424 80°C.

425 RD cells were seeded in T75 flasks, cultured for 24 h at 37°C with 5% CO₂ and
426 transduced with lentiviral particles harboring KLK13, TMPRSS2 gene or control vector in the
427 presence of polybrene (4 μ g/ml; Sigma-Aldrich, Poland). Cells were further cultured for 72 h
428 at 37°C with 5% CO₂ and positively transduced cells were selected using blasticidin (2 μ g/ml
429 Sigma-Aldrich, Poland). Primary human epithelial cells seeded on 10 cm² dishes were cultured
430 in BEGM medium and transduced with lentiviral particles harboring shRNA against KLK13 (a

431 set of 3) or GFP gene in the presence of polybrene (5 µg/ml; Sigma-Aldrich, Poland). Cells
432 were further cultured for 72 h at 37°C with 5% CO₂ and positively transduced cells were
433 selected using puromycin (5 µg/ml Sigma-Aldrich, Poland). Selected cells were plated on insert
434 supports and further cultured in ALI in the presence of puromycin (1 µg/ml).

435

436 **Pseudoviruses**

437 293T cells were seeded on 6-wells plates, cultured for 24 h at 37°C with 5% CO₂ and
438 transfected using polyethyleneimine (Sigma-Aldrich, Poland) with the lentiviral packaging
439 plasmid (psPAX), the VSV-G envelope plasmid (pMD2G) or HCoV-HKU1 S glycoprotein
440 (pCAGGS-HKU1-S) and third plasmid encoding luciferase (pRR Luciferase). pRR Luciferase
441 was a gift from Paul Khavari (Addgene plasmid # 120798) (97). Cells were further cultured for
442 72 h at 37°C with 5% CO₂ and pseudoviruses were collected every 24 h and stored at 4°C.

443 RD cells were seeded in 48-wells plates, cultured for 24 h at 37°C with 5% CO₂ and
444 transduced with pseudoviruses harboring VSV-G or S-HKU1 proteins or lacking the fusion
445 protein (Δ Env) in the presence of polybrene (4 µg/ml; Sigma-Aldrich, Poland). HAE cultures
446 were washed thrice with 100 µl of 1 × PBS and subsequently inoculated with S-HKU1 or VSV-
447 G pseudoviruses. After 4 h incubation at 37°C unbound virions were removed by washing with
448 100 µl of 1 × PBS and HAE cultures were cultured at an air-liquid interphase. Cells were further
449 cultured for 72 h at 37°C with 5% CO₂ and lysed in luciferase substrate buffer (Bright-Glo;
450 Promega, Poland). Lysates were transferred onto white 96-wells plates and luciferase levels
451 were measured on a microplate reader Gemini EM (Molecular Devices, UK).

452

453 **Isolation of nucleic acids and reverse transcription (RT)**

454 Viral DNA/RNA Kit (A&A Biotechnology, Poland) was used for nucleic acid isolation
455 from cell culture supernatants, according to the manufacturer's instructions. Cellular RNA was

456 isolated using Fenzol reagent (A&A Biotechnology, Poland), followed by DNase I treatment
457 (Thermo Fisher Scientific, Poland). cDNA samples were prepared with a High Capacity cDNA
458 Reverse Transcription Kit (Thermo Fisher Scientific, Poland), according to the manufacturer's
459 instructions.

460

461 **PCR**

462 Human KLKs mRNA was reverse transcribed and amplified in a reaction mixture
463 containing 1 × Dream *Taq* Green PCR master mix (Thermo Fisher Scientific, Poland) and
464 appropriate primers (**Table 3**; 500 nM each). β -actin was used as a household gene reference.
465 The reaction was carried out according to the scheme: 5 min at 95°C, followed by 35 cycles of
466 30 s at 95°C, 20 s at 59°C and 20 s at 72°C, followed by 10 min at 72°C.

467

468 **Quantitative PCR (qPCR)**

469 HCoV-HKU1 RNA yield was assessed using real-time PCR (7500 Fast Real-Time
470 PCR; Life Technologies, Poland). cDNA was amplified in a reaction mixture containing
471 1 × TaqMan Universal PCR Master Mix (Thermo Fisher Scientific, Poland), in the presence of
472 FAM / TAMRA (6-carboxyfluorescein / 6-carboxytetramethylrhodamine) probe (100 nM; 5' –
473 TTGAAGGCTCAGGAAGGTCTGCTTCTAA– 3') and primers (450 nM each; forward: 5' –
474 CTGGTACGATTTTGCCTCAA – 3' and reverse: 5' -ATTATTGGGTCCACGTGATTG– 3')
475 (98). The reaction was carried out according to the scheme: 2 min at 50°C and 10 min at 92°C,
476 followed by 40 cycles of 15 s at 92°C and 1 min at 60°C.

477

478 **Detection of HCoV-HKU1 N sg mRNA**

479 Total nucleic acids were isolated from virus or mock-infected cells at 7 days p.i. using
480 Fenzol reagent (A&A Biotechnology, Poland), according to the manufacturer's instructions.

481 Reverse transcription was performed using a high-capacity cDNA reverse transcription kit (Life
482 Technologies, Poland), according to the manufacturer's instructions. Viral cDNA was
483 amplified in a 20 µl reaction mixture containing 1 × Dream *Taq* Green PCR master mix
484 (Thermo Fisher Scientific, Poland), and primers (500 nM each). The following primers were
485 used to amplify HCoV-HKU1 subgenomic mRNA (sg mRNA): common sense primer (leader
486 sequence), 5' – TCTTGTCAGATCTCATTAATCTAAACT -3'; nucleocapsid antisense for
487 1st PCR, 5' – AACTCCTTGACCATCTGAAAATTT – 3'; nucleocapsid antisense for nested
488 PCR, 5' – AGGAATAATGTGGGATAGTATTT – 3'. The conditions were as follows: 3 min
489 at 95°C, 35 cycles (30 cycles for nested PCR) of 30 s at 95°C, 30 s at 49°C, and 20 s at 72°C,
490 followed by 5 min at 72°C and 10 min at 4°C. The PCR products were run on 1% agarose gels
491 (1Tris-acetate EDTA [TAE] buffer) and analyzed using molecular imaging software (Thermo
492 Fisher Scientific, Poland).

493

494 **Detection of TMPRSS2 protease**

495 After blasticidin selection, RD cells expressing TMPRSS2 (RD_TMPRSS2), KLK13
496 (RD_KLK13) or control cells (RD_ctrl) were scraped and collected by centrifugation. Cells
497 were lysed in RIPA buffer (50 mM Tris, 150 mM NaCl, 1% Nonidet P-40, 0.5% sodium
498 deoxycholate, 0.1% SDS, pH 7.5), boiled for 5 min, cooled on ice, and separated on 10%
499 polyacrylamide gel alongside dual-color Page Ruler Prestained Protein size markers (Thermo
500 Fisher Scientific, Poland). The separated proteins were then transferred onto a Westran S PVDF
501 membrane (GE Healthcare, Poland) by wet blotting (Bio-Rad, Poland) for 1 h, 100 Volts in
502 transfer buffer (25 mM Tris, 192 mM glycine, 20% methanol) at 4°C. The membranes were
503 blocked by overnight incubation at 4°C in TBS-Tween (0.1%) buffer supplemented with 5%
504 skimmed milk (BioShop, Canada). A mouse monoclonal anti-TMPRSS2 antibody (clone
505 P5H9-A3; 1:500 dilution; Sigma-Aldrich, Poland), followed by incubation with a horseradish

506 peroxidase-labeled anti-mouse IgG (65 ng/ml; Dako, Denmark) diluted in 5% skimmed
507 milk / TBS-Tween (0.1%). The signal was developed using the Pierce ECL Western blotting
508 substrate (Thermo Scientific, Poland) and visualized using the ChemiDoc Imaging System
509 (Bio-Rad, Poland).

510

511 **Expression and purification of KLK13 and KLK14**

512 The proKLK13 gene was amplified using cDNA obtained from HAE cultures and
513 specific primers. The codon-optimized proKLK14 gene was custom-synthesized (Thermo
514 Scientific, Poland). The products were cloned into the pLEXSY_I-blecherry3 plasmid (Jena
515 Bioscience, Germany) and the resulting constructs were verified by sequencing. All
516 preparations for transfection, selection, and expression of the host *Leishmania tarentolae* strain
517 T7-TR were performed according to the Jena Bioscience protocol for inducible expression of
518 recombinant proteins secreted to medium (LEXSinduce Expression kit, Jena Bioscience,
519 Germany). Expression of proKLK13 and proKLK14 was induced with 15 µg/ml of tetracycline
520 (BioShop, Canada) and carried out for 3 consecutive days. Culture media were collected and
521 precipitated with 80% ammonium sulfate, spun down at 15,000 × g for 30 min at 4°C. Pellets
522 were suspended in 10mM sodium phosphate pH 7.5 and dialyzed overnight at 4°C into 10mM
523 sodium phosphate pH 7.5. The KLKs were isolated *via* the 6 × His tag using nickel resin (GE
524 Healthcare, Poland) according to the manufacturer's protocol. Obtained fractions were
525 analyzed by SDS PAGE in reducing conditions and fractions containing proKLK13 or
526 proKLK14 were concentrated with Vivaspin® 2 (Sartorius, Germany) and further purified
527 using size exclusion chromatography (Superdex s75 pg; GE Healthcare, Poland). Fractions
528 containing proKLK13 or proKLK14 were concentrated and the buffer was changed to 50mM
529 Tris pH 7.5, 150 mM NaCl. After purification and self-activation at 37°C for 24 h, activity of

530 proteases was assessed by serine protease inhibitor Kazal-type 6 (SPINK6) titration, as
531 described previously (63).

532

533 **Cloning of HmuY-based CleavEx fusion proteins**

534 The fusion constructs were based on positions 26-216 of the *Porphyromonas gingivalis*
535 HmuY protein-encoding gene (accession number ABL74281.1), employed as a carrier protein.
536 The gene was amplified using Phusion DNA polymerase (Thermo Scientific, Poland) and
537 specific primers (forward: 5' – ATATGCGGCCGCGACGAGCCGAACCAACCCTCCA –
538 3' and reverse: 5' – ATACTCGAGTTATTTAACGGGGTATGTATAAGCGAAAGTGA –
539 3') from whole-genomic DNA isolated from *Porphyromonas gingivalis* strain W83. PCR
540 conditions were as follows: 98°C for 30s, followed by denaturation at 98°C for 10s, annealing
541 at 68°C for 40s and extension at 72°C for 30s/kb over 35 cycles with a final extension at 72°C
542 for 7 min. Then, the HmuY gene was further amplified in the three consecutive PCR reactions
543 with primers specific to the 5' HmuY fragment and 3'-specific primer introducing additional
544 nucleotides dependent on the designed sequence (proKLLK13 primers, **Table 4**). The reaction
545 was ligated into a modified pETDuet plasmid (potential tryptic cleavage sites were removed
546 from the MCS) using Quick Change mutagenesis using Phusion DNA polymerase (Thermo
547 Scientific, Poland). Alternatively, the designed fusion protein-encoding sequences were
548 produced using Phusion Site-Directed Mutagenesis (Thermo Scientific, Poland), *via* sequence
549 exchange of the previously prepared CleavEx construct (HKU1-S primers, **Table 4**). The final
550 product was transformed into competent *E. coli* T10 cells and further purified and sequenced.

551

552 **Expression and purification of CleavEx fusion proteins**

553 Protein expression was performed in *E. coli* BL21 and was induced by the addition of
554 0.5 mM IPTG to the bacterial culture (OD₆₀₀ 0.5-0.6), followed by shaking for 3h at 37°C.

555 Then, the bacteria were spun down and the pellet was suspended in buffer A (10 mM sodium
556 phosphate, 500 mM NaCl and 5 mM imidazole, pH 7.4). The pellet suspension was then
557 sonicated and spun down. Soluble proteins were purified using HisTrapTM Excel (GE
558 Healthcare, Poland) column in buffer A with a linear gradient of 0-100% of 1 M imidazole in
559 buffer A in 20 column volumes. Fractions containing protein of interest were pooled together
560 and the buffer was exchanged to 50 mM Tris pH 7.5. Lastly, the protein of interest was purified
561 by ion-exchange chromatography using MonoQ 4.6/100 PE column (GE Healthcare, Poland)
562 with a linear gradient of 0-100% 50 mM Tris pH 7.5, 1M NaCl in 15 column volumes.

563

564 **Expression and purification of the HCoV-HKU1 Spike protein**

565 293T cells were seeded on 60 cm² dishes, cultured for 24 h at 37°C with 5% CO₂ and
566 transfected with 25 µg of pSecTag2-HKU-S plasmid per dish using polyethyleneimine (Sigma
567 Aldrich, Poland). Cells were further cultured for 72 h at 37°C with 5% CO₂ and collected for
568 HKU1-S purification. Cell pellets were lysed in RIPA buffer (50 mM Tris, 150 mM NaCl,
569 1% Nonidet P-40, 0.5% sodium deoxycholate, 0.1% SDS, pH 7.5) in the presence of Viscolase
570 (1250 U/ml; A&A Biotechnology, Poland), clarified by centrifugation, and filtered (0.45 µm
571 syringe PES filter). Supernatant containing 6 × His tagged S protein was mixed in 1:2 ratio with
572 binding buffer (20 mM NaH₂PO₄, 500 mM NaCl, 20 mM imidazole, pH = 7.4) and purified
573 using a fast performance liquid chromatography system (FPLC; AKTA, GE Healthcare,
574 Poland) with a Ni²⁺ HiTrap IMAC (2 × 1 ml) column (GE Healthcare, Poland) preequilibrated
575 with the binding buffer. The 6 × His tagged S protein was eluted with elution buffer (20 mM
576 NaH₂PO₄, 500 mM NaCl, 500 mM imidazole, pH = 6.9). The control sample from mock-
577 transfected cells was prepared in the same manner. Fractions containing 6 × His tagged
578 S protein or the respective fractions from control purification were pooled and dialyzed against
579 phosphate-buffered saline (PBS) with 5% glycerol.

580

581 **CleavEx screening assay and HKU1-S cleavage**

582 A total of 15 ng of each CleavEx protein was incubated with 50, 250 and 500 nM
583 KLK13, respectively in 50 mM Tris pH 7.5. For the full-length Spike protein, fractions
584 containing purified HKU1-S or mock samples were incubated with 0.5, 1.0 or 5.0 μ M KLK13,
585 respectively in 50 mM Tris pH 7.5. Samples were incubated at 37°C for 3 hours and
586 immediately halted with the addition of 50 mM DTT-supplemented SDS sample buffer (1:1),
587 boiled for 5 min, cooled on ice, and separated on 10% polyacrylamide gels alongside dual-color
588 Page Ruler Prestained Protein size markers (Thermo Fisher Scientific, Poland). The separated
589 proteins were then transferred onto a Westran S PVDF membrane (GE Healthcare, Poland) by
590 wet blotting (Bio-Rad, Poland) for 1 h, 100 Volts in transfer buffer: 25 mM Tris, 192 mM
591 glycine, 20% methanol at 4°C. The membranes were then blocked by overnight incubation (at
592 4°C) in TBS-Tween (0.1%) buffer supplemented with 5% skimmed milk (BioShop, Canada).
593 A horseradish peroxidase-labeled anti-His tag antibody (1:25000 dilution; Sigma-Aldrich,
594 Poland) diluted in 5% skimmed milk / TBS-Tween (0.1%) was used to detect the His-tagged
595 HmuY proteins. The signal was developed using the Pierce ECL Western blotting substrate
596 (Thermo Scientific, Poland) and visualized using the ChemiDoc Imaging System (Bio-Rad,
597 Poland).

598

599 **Identification of the cleavage site**

600 A total of 10 μ g S1/S2 CleavEx protein was incubated with 500 nM of KLK13 at 37°C
601 for 5 h. Next, the reaction was stopped by the addition of 50 mM DTT-supplemented SDS
602 sample buffer (1:1) and samples were immediately boiled for 5 min. The samples were then
603 separated on 10% polyacrylamide gel alongside the dual-color Page Ruler Prestained Protein
604 size markers (Thermo Fisher Scientific, Poland) in the Tris-Tricine SDS-PAGE system. The

605 separated proteins were then electrotransferred onto a Western S PVDF membrane (GE
606 Healthcare, Poland) using the Trans-Blot SD Semi-Dry Transfer Cell (Bio-Rad, Poland). The
607 transfer was performed for 30 min at 15 V in transfer buffer (10 mM N-cyclohexyl-3-
608 aminopropanesulfonic acid , 10% methanol, pH 11). Following the transfer, the membrane was
609 stained with 0.025% (w/v) Coomassie Brilliant Blue R-250 (BioShop, Poland) and the bands
610 of interest were sequenced *via* Edman degradation using a PPSQ-31A automatic protein
611 sequencer (Shimadzu, Japan).

612

613 **TABLES**

614 **Table 1. KLKs inhibitors used in the study (61).**

Protein	Inhibitor sequences
KLK7	Biotin-KTLF-CMK / Biotin-PEG-KTLF-CMK
KLK8	Biotin-TNKR-CMK / Biotin-PEG-TNKR-CMK
KLK13	Biotin-VRFR-CMK / Biotin-PEG-VRFR-CMK

615

616 **Table 2. Primers used for generation of plasmid constructs.**

Target/vector	Primer	Primer sequence (5'– 3')
KLK13/ pWPI	Sense	AGTCGTTTAAACGCCACCATGTGGCCCCTGGCCCTAGTGA TCGCC
	Antisense	GATCGTTTAAACTTATTGTGGGCCCTTCAACCATTTT TG
TMPRSS2/ pWPI	Sense	AGTCGTTTAAACGCCACCATGGCTTTGAACTCAGGG TCACCA
	Antisense	GATCGTTTAAACTTAGCCGTCTGCCCTCATTTGTCGA TAAATC
shRNA1 for KLK13/ pLKO.1-TRC	Sense	CCGGAACAGAACACTGTATGGCATCCTCGAGGATGC CATAACAGTGTCTGTTTTTTTG
	Antisense	AATTCAAAAAACAGAACACTGTATGGCATCCTCGA GGATGCCATACAGTGTCTGTT
shRNA2 for KLK13/ pLKO.1-TRC	Sense	CCGGAACACTCTACAATGTGCCAACATCTCGAGATGTT GGCACATTGTAGAGTTTTTTTG
	Antisense	AATTCAAAAAAACTCTACAATGTGCCAACATCTCGA GATGTTGGCACATTGTAGAGTT
shRNA3 for KLK13/ pLKO.1-TRC	Sense	CCGGAACATGTTGTGTGCCGGCACACTCGAGTGTGC CGGCACACAACATGTTTTTTTG
	Antisense	AATTCAAAAAAACATGTTGTGTGCCGGCACACTCGA GTGTGCCGGCACACAACATGT
KLK13/ pLEXY	Sense 1	GACGACGACAAGCTTGGTGACGTTGCCAATGCTGTG
	Sense 2	CCATCATCACCACGACGACGACGACAAGCTTGGTGA CGTTG
	Sense 3	ATATCTAGACATCACCATCATCACCACGACGACGAC
	Antisense	ATAGCGGCCGCTTATTGTGGGCCCTTCAACCAT
HKU1-S/ pSecTag2	Sense	AGCTGGCCCAGCCGGCCCTGCTGATCATCTTCATCCT G
	Antisense	AGCTGCGGCCGCAGCGTAATCTGGAACATCGTATGG GTAGCTGTAGCCCTGGCGGACCC

617

618 **Table 3. Primers used for PCR of each KLK gene.**

Target	Primer	Primer sequence (5'– 3')
KLK1	Sense	CTCCTGGAGAACCACACCCGCC
	Antisense	GCGACAGAAGGCTTATTGGGGG
KLK2	Sense	GGCAGGTGGCTGTGTACAGTC
	Antisense	CAACATGAACTCTGTCACCTTCTC
KLK3	Sense	CGATATGAGCCTCCTGAAGAATC
	Antisense	TACCTTGAAGCACACCATTACA
KLK4	Sense	GCGGCACTGGTCATGGAAAACG
	Antisense	AACATGCTGGGGTGGTACAGCGG
KLK5	Sense	GTCACCAGTTTATGAATCTGGGC
	Antisense	GGCGCAGAACATGGTGTTCATC
KLK6	Sense	GAAGCTGATGGTGGTGGTGGTCTG
	Antisense	GTCAGGGAAATCACCATCTGCTGTC
KLK7	Sense	CCGCCCACTGCAAGATGAATGAG
	Antisense	AGCGCACAGCATGGAATTTTCC
KLK8	Sense	GCCTTGTTCCAGGGCCAGC
	Antisense	GCATCCTCACACTTCTTCTGGG
KLK9	Sense	TCTTCCCCACCCTGGCTTCAAC
	Antisense	CGGGGTCTGGAGCAGGGCTCAG
KLK10	Sense	GGAAACAAGCCACTGTGGGC
	Antisense	GAGGATGCCTTGGAGGGTCTC
KLK11	Sense	CTCTGGCAACAGGGCTTGTAGGG
	Antisense	GCATCGCAAGGTGTGAGGCAGG
KLK12	Sense	TTGACCACAGGTGGGTCTCTCA
	Antisense	GTGTAGACTCCAGGGATGCCA
KLK13	Sense	GGAGAAGCCCCACCCACCTG
	Antisense	CACGGATCCACAGGACGTATCTTG
KLK14	Sense	CACTGCGGCCGCCGATC
	Antisense	GGCAGGGCGCAGCGCTCC
KLK15	Sense	CTACGGACCACGTCTCGGGTC
	Antisense	GACACCAGGCTTGGTGGTGTG
β-actin	Sense	CCCACTGTGCCATCTACG
	Antisense	AGGATCTTCATGAGGTAGTCAGTCAG

619 Primers for KLKs: 1, 2, 4-15 were acquired from (99). Primers for KLK3 were developed and
 620 optimized in our laboratory.

621 **Table 4. Primers used in the CleavEx design.**

Target	Primer	Primer sequence (5'– 3')
proKLK13	Antisense	ATATGCGGCCGCTTATTTAACGGGGTATGTATAAGCGA
	Sense 1	TGCTGAACACCAACGACGAGCCGAACCAACCCT
	Sense 2	AAGCAGCAAAGTGCTGAACACCAACGACGAGCC
	Sense 3	ATATGTCGACCAGGAAAGCAGCAAAGTGCTGAACACCAAC
HKU1-S (S1/S2)	Antisense	GTCGACCTGCAGGCTCGC
	Sense	CGTAAACGTCGTTCTATCTCTGCGGACGAGCCGAACCAACCC
HKU1-S (S2/S2')	Antisense	GTCGACCTGCAGGCTCGC
	Sense	TCTTCTTCTCGTTCTTTTTTTGAAGACGAGCCGAACCAACCC

622

623 **ACKNOWLEDGEMENTS**

624 This work was supported by grants from the National Science Center UMO-
625 2013/08/W/NZ1/00696 (J.P.), UMO-2016/22/E/NZ5/00332 (T.K.), UMO-
626 2013/08/S/NZ6/00730 (A.N.), UMO-2012/07/E/NZ6/01712 and UMO-2017/27/B/NZ6/02488
627 (K.P.). Faculty of Biochemistry, Biophysics and Biotechnology of the Jagiellonian University
628 is a partner of the Leading National Research Center supported by the Ministry of Science and
629 Higher Education of the Republic of Poland. The authors are grateful to Xingchuan Huang for
630 providing pCAGGS/HKU1-S plasmid, Ambra Saraccino for providing pWPI vector, Laura
631 Sasiadek for providing KLK primers used in the study and Grzegorz Dubin for providing
632 reference samples. The funders had no role in study design, data collection, and analysis,
633 decision to publish, or preparation of the manuscript.

634

635 **AUTHOR CONTRIBUTIONS STATEMENT**

636 A.M., K.F., E.B., M.K, A.N. and P.M conducted the experiments. A.L., T.K., M.O., M.U. and
637 J.P. provided materials and methods for the study. A.M. and K.P. designed the study and
638 experiments, analyzed the data, and wrote the manuscript. K.P. and T.K. supervised the study.
639 All authors reviewed the manuscript and approved the submitted version. All authors agreed to
640 be personally accountable for their contributions and to ensure that questions related to the
641 accuracy or integrity of any part of the work are appropriately investigated, resolved, and the
642 resolution documented in the literature.

643

644 **ADDITIONAL INFORMATION**

645 **Competing interests**

646 The authors declare no competing financial interests.

647

648 REFERENCES

- 649 1. B. N. Fields, D. M. Knipe, P. M. Howley, *Fields virology*. (Wolters Kluwer Health/Lippincott
650 Williams & Wilkins, Philadelphia, ed. 6th ed, 2013).
- 651 2. J. S. Peiris, K. Y. Yuen, A. D. Osterhaus, K. Stöhr, The severe acute respiratory syndrome. *N*
652 *Engl J Med* **349**, 2431-2441 (2003); published online EpubDec (10.1056/NEJMra032498).
- 653 3. R. J. de Groot, S. C. Baker, R. S. Baric, C. S. Brown, C. Drosten, L. Enjuanes, R. A. Fouchier, M.
654 Galiano, A. E. Gorbalenya, Z. A. Memish, S. Perlman, L. L. Poon, E. J. Snijder, G. M. Stephens,
655 P. C. Woo, A. M. Zaki, M. Zambon, J. Ziebuhr, Middle East respiratory syndrome coronavirus
656 (MERS-CoV): announcement of the Coronavirus Study Group. *J Virol* **87**, 7790-7792 (2013);
657 published online EpubJul (10.1128/JVI.01244-13).
- 658 4. A. M. Zaki, S. van Boheemen, T. M. Bestebroer, A. D. Osterhaus, R. A. Fouchier, Isolation of a
659 novel coronavirus from a man with pneumonia in Saudi Arabia. *N Engl J Med* **367**, 1814-1820
660 (2012); published online EpubNov 8 (10.1056/NEJMoa1211721).
- 661 5. L. van der Hoek, K. Pyrc, M. F. Jebbink, W. Vermeulen-Oost, R. J. Berkhout, K. C. Wolthers, P.
662 M. Wertheim-van Dillen, J. Kaandorp, J. Spaargaren, B. Berkhout, Identification of a new
663 human coronavirus. *Nat Med* **10**, 368-373 (2004); published online EpubApr
664 (10.1038/nm1024).
- 665 6. L. van der Hoek, K. Sure, G. Ihorst, A. Stang, K. Pyrc, M. F. Jebbink, G. Petersen, J. Forster, B.
666 Berkhout, K. Uberla, Croup is associated with the novel coronavirus NL63. *PLoS Med* **2**, e240
667 (2005); published online EpubAug (10.1371/journal.pmed.0020240).
- 668 7. C. L. Yeager, R. A. Ashmun, R. K. Williams, C. B. Cardellicchio, L. H. Shapiro, A. T. Look, K. V.
669 Holmes, Human aminopeptidase N is a receptor for human coronavirus 229E. *Nature* **357**,
670 420-422 (1992); published online EpubJun (10.1038/357420a0).
- 671 8. R. Dijkman, M. F. Jebbink, M. Deijns, A. Milewska, K. Pyrc, E. Buelow, A. van der Bijl, L. van der
672 Hoek, Replication-dependent downregulation of cellular angiotensin-converting enzyme 2
673 protein expression by human coronavirus NL63. *J Gen Virol* **93**, 1924-1929 (2012); published
674 online EpubSep (10.1099/vir.0.043919-0).
- 675 9. H. Hofmann, K. Pyrc, L. van der Hoek, M. Geier, B. Berkhout, S. Pöhlmann, Human
676 coronavirus NL63 employs the severe acute respiratory syndrome coronavirus receptor for
677 cellular entry. *Proc Natl Acad Sci U S A* **102**, 7988-7993 (2005); published online EpubMay
678 (10.1073/pnas.0409465102).
- 679 10. S. Pöhlmann, T. Gramberg, A. Wegele, K. Pyrc, L. van der Hoek, B. Berkhout, H. Hofmann,
680 Interaction between the spike protein of human coronavirus NL63 and its cellular receptor
681 ACE2. *Adv Exp Med Biol* **581**, 281-284 (2006)10.1007/978-0-387-33012-9_47).
- 682 11. H. Hofmann, A. Marzi, T. Gramberg, M. Geier, K. Pyrc, L. van der Hoek, B. Berkhout, S.
683 Pöhlmann, Attachment factor and receptor engagement of SARS coronavirus and human
684 coronavirus NL63. *Advances in experimental medicine and biology* **581**, 219-227
685 (2006)10.1007/978-0-387-33012-9_37).
- 686 12. A. Naskalska, A. Dabrowska, P. Nowak, A. Szczepanski, K. Jasik, A. Milewska, M. Ochman, S.
687 Zeglen, Z. Rajfur, K. Pyrc, Novel coronavirus-like particles targeting cells lining the respiratory
688 tract. *PLoS One* **13**, e0203489 (2018)10.1371/journal.pone.0203489).
- 689 13. A. Naskalska, A. Dabrowska, A. Szczepanski, A. Milewska, K. P. Jasik, K. Pyrc, Membrane
690 protein of HCoV-NL63 is responsible for interaction with the adhesion receptor. *J Virol*,
691 (2019); published online EpubJul 17 (10.1128/JVI.00355-19).
- 692 14. A. Milewska, M. Zarebski, P. Nowak, K. Stozek, J. Potempa, K. Pyrc, Human coronavirus NL63
693 utilizes heparan sulfate proteoglycans for attachment to target cells. *J Virol* **88**, 13221-13230
694 (2014); published online EpubNov (10.1128/JVI.02078-14).
- 695 15. W. Li, M. J. Moore, N. Vasilieva, J. Sui, S. K. Wong, M. A. Berne, M. Somasundaran, J. L.
696 Sullivan, K. Luzuriaga, T. C. Greenough, H. Choe, M. Farzan, Angiotensin-converting enzyme 2
697 is a functional receptor for the SARS coronavirus. *Nature* **426**, 450-454 (2003); published
698 online EpubNov (10.1038/nature02145).

- 699 16. V. S. Raj, H. Mou, S. L. Smits, D. H. Dekkers, M. A. Müller, R. Dijkman, D. Muth, J. A. Demmers,
700 A. Zaki, R. A. Fouchier, V. Thiel, C. Drosten, P. J. Rottier, A. D. Osterhaus, B. J. Bosch, B. L.
701 Haagmans, Dipeptidyl peptidase 4 is a functional receptor for the emerging human
702 coronavirus-EMC. *Nature* **495**, 251-254 (2013); published online EpubMar
703 (10.1038/nature12005).
- 704 17. R. Vlasak, W. Luytjes, W. Spaan, P. Palese, Human and bovine coronaviruses recognize sialic
705 acid-containing receptors similar to those of influenza C viruses. *Proc Natl Acad Sci U S A* **85**,
706 4526-4529 (1988); published online EpubJun (
- 707 18. A. Szczepanski, K. Owczarek, M. Bzowska, K. Gula, I. Drebot, M. Ochman, B. Maksym, Z.
708 Rajfur, J. A. Mitchell, K. Pyrc, Canine Respiratory Coronavirus, Bovine Coronavirus, and
709 Human Coronavirus OC43: Receptors and Attachment Factors. *Viruses* **11**, (2019); published
710 online EpubApr (10.3390/v11040328).
- 711 19. P. C. Woo, S. K. Lau, C. M. Chu, K. H. Chan, H. W. Tsoi, Y. Huang, B. H. Wong, R. W. Poon, J. J.
712 Cai, W. K. Luk, L. L. Poon, S. S. Wong, Y. Guan, J. S. Peiris, K. Y. Yuen, Characterization and
713 complete genome sequence of a novel coronavirus, coronavirus HKU1, from patients with
714 pneumonia. *J Virol* **79**, 884-895 (2005); published online EpubJan (10.1128/JVI.79.2.884-
715 895.2005).
- 716 20. S. R. Dominguez, C. C. Robinson, K. V. Holmes, Detection of four human coronaviruses in
717 respiratory infections in children: a one-year study in Colorado. *J Med Virol* **81**, 1597-1604
718 (2009); published online EpubSep (10.1002/jmv.21541).
- 719 21. W. Zhou, W. Wang, H. Wang, R. Lu, W. Tan, First infection by all four non-severe acute
720 respiratory syndrome human coronaviruses takes place during childhood. *BMC Infect Dis* **13**,
721 433 (2013); published online EpubSep (10.1186/1471-2334-13-433).
- 722 22. R. Dijkman, M. F. Jebbink, S. M. Koekkoek, M. Deijis, H. R. Jónsdóttir, R. Molenkamp, M.
723 leven, H. Goossens, V. Thiel, L. van der Hoek, Isolation and characterization of current human
724 coronavirus strains in primary human epithelial cell cultures reveal differences in target cell
725 tropism. *J Virol* **87**, 6081-6090 (2013); published online EpubJun (10.1128/JVI.03368-12).
- 726 23. S. R. Dominguez, S. Shrivastava, A. Berglund, Z. Qian, L. G. Góes, R. A. Halpin, N. Fedorova, A.
727 Ransier, P. A. Weston, E. L. Durigon, J. A. Jerez, C. C. Robinson, C. D. Town, K. V. Holmes,
728 Isolation, propagation, genome analysis and epidemiology of HKU1 betacoronaviruses. *J Gen
729 Virol* **95**, 836-848 (2014); published online EpubApr (10.1099/vir.0.059832-0).
- 730 24. S. R. Dominguez, E. A. Travanty, Z. Qian, R. J. Mason, Human coronavirus HKU1 infection of
731 primary human type II alveolar epithelial cells: cytopathic effects and innate immune
732 response. *PLoS One* **8**, e70129 (2013)10.1371/journal.pone.0070129).
- 733 25. K. Pyrc, A. C. Sims, R. Dijkman, M. Jebbink, C. Long, D. Deming, E. Donaldson, A. Vabret, R.
734 Baric, L. van der Hoek, R. Pickles, Culturing the unculturable: human coronavirus HKU1
735 infects, replicates, and produces progeny virions in human ciliated airway epithelial cell
736 cultures. *J Virol* **84**, 11255-11263 (2010); published online EpubNov (10.1128/JVI.00947-10).
- 737 26. X. Huang, W. Dong, A. Milewska, A. Golda, Y. Qi, Q. K. Zhu, W. A. Marasco, R. S. Baric, A. C.
738 Sims, K. Pyrc, W. Li, J. Sui, Human Coronavirus HKU1 Spike Protein Uses O-Acetylated Sialic
739 Acid as an Attachment Receptor Determinant and Employs Hemagglutinin-Esterase Protein
740 as a Receptor-Destroying Enzyme. *J Virol* **89**, 7202-7213 (2015); published online EpubJul
741 (10.1128/JVI.00854-15).
- 742 27. M. J. Bakkers, Y. Lang, L. J. Feitsma, R. J. Hulswit, S. A. de Poot, A. L. van Vliet, I. Margine, J. D.
743 de Groot-Mijnes, F. J. van Kuppeveld, M. A. Langereis, E. G. Huizinga, R. J. de Groot,
744 Betacoronavirus Adaptation to Humans Involved Progressive Loss of Hemagglutinin-Esterase
745 Lectin Activity. *Cell Host Microbe* **21**, 356-366 (2017); published online EpubMar 8
746 (10.1016/j.chom.2017.02.008).
- 747 28. R. J. G. Hulswit, Y. Lang, M. J. G. Bakkers, W. Li, Z. Li, A. Schouten, B. Ophorst, F. J. M. van
748 Kuppeveld, G. J. Boons, B. J. Bosch, E. G. Huizinga, R. J. de Groot, Human coronaviruses OC43
749 and HKU1 bind to 9-. *Proc Natl Acad Sci U S A* **116**, 2681-2690 (2019); published online
750 EpubFeb (10.1073/pnas.1809667116).

- 751 29. T. M. Gallagher, C. Escarmis, M. J. Buchmeier, Alteration of the pH dependence of
752 coronavirus-induced cell fusion: effect of mutations in the spike glycoprotein. *J Virol* **65**,
753 1916-1928 (1991); published online EpubApr (
754 30. R. Nomura, A. Kiyota, E. Suzuki, K. Kataoka, Y. Ohe, K. Miyamoto, T. Senda, T. Fujimoto,
755 Human coronavirus 229E binds to CD13 in rafts and enters the cell through caveolae. *J Virol*
756 **78**, 8701-8708 (2004); published online EpubAug (10.1128/JVI.78.16.8701-8708.2004).
757 31. Y. Inoue, N. Tanaka, Y. Tanaka, S. Inoue, K. Morita, M. Zhuang, T. Hattori, K. Sugamura,
758 Clathrin-dependent entry of severe acute respiratory syndrome coronavirus into target cells
759 expressing ACE2 with the cytoplasmic tail deleted. *J Virol* **81**, 8722-8729 (2007); published
760 online EpubAug (10.1128/JVI.00253-07).
761 32. E. Van Hamme, H. L. Dewerchin, E. Cornelissen, B. Verhasselt, H. J. Nauwynck, Clathrin- and
762 caveolae-independent entry of feline infectious peritonitis virus in monocytes depends on
763 dynamin. *J Gen Virol* **89**, 2147-2156 (2008); published online EpubSep
764 (10.1099/vir.0.2008/001602-0).
765 33. H. Wang, P. Yang, K. Liu, F. Guo, Y. Zhang, G. Zhang, C. Jiang, SARS coronavirus entry into host
766 cells through a novel clathrin- and caveolae-independent endocytic pathway. *Cell Res* **18**,
767 290-301 (2008); published online EpubFeb (10.1038/cr.2008.15).
768 34. A. Milewska, P. Nowak, K. Owczarek, A. Szczepanski, M. Zarebski, A. Hoang, K. Berniak, J.
769 Wojarski, S. Zeglen, Z. Baster, Z. Rajfur, K. Pyrc, Entry of Human Coronavirus NL63 into the
770 Cell. *J Virol* **92**, (2018); published online EpubFeb (10.1128/JVI.01933-17).
771 35. K. Owczarek, A. Szczepanski, A. Milewska, Z. Baster, Z. Rajfur, M. Sarna, K. Pyrc, Early events
772 during human coronavirus OC43 entry to the cell. *Sci Rep* **8**, 7124 (2018); published online
773 EpubMay 8 (10.1038/s41598-018-25640-0).
774 36. J. E. Park, D. J. Cruz, H. J. Shin, Receptor-bound porcine epidemic diarrhea virus spike protein
775 cleaved by trypsin induces membrane fusion. *Arch Virol* **156**, 1749-1756 (2011); published
776 online EpubOct (10.1007/s00705-011-1044-6).
777 37. C. A. de Haan, B. J. Haijema, P. Schellen, P. Wichgers Schreur, E. te Lintelo, H. Vennema, P. J.
778 Rottier, Cleavage of group 1 coronavirus spike proteins: how furin cleavage is traded off
779 against heparan sulfate binding upon cell culture adaptation. *J Virol* **82**, 6078-6083 (2008);
780 published online EpubJun (10.1128/JVI.00074-08).
781 38. R. N. Kirchdoerfer, C. A. Cottrell, N. Wang, J. Pallesen, H. M. Yassine, H. L. Turner, K. S.
782 Corbett, B. S. Graham, J. S. McLellan, A. B. Ward, Pre-fusion structure of a human coronavirus
783 spike protein. *Nature* **531**, 118-121 (2016); published online EpubMar
784 (10.1038/nature17200).
785 39. C. A. de Haan, K. Stadler, G. J. Godeke, B. J. Bosch, P. J. Rottier, Cleavage inhibition of the
786 murine coronavirus spike protein by a furin-like enzyme affects cell-cell but not virus-cell
787 fusion. *J Virol* **78**, 6048-6054 (2004); published online EpubJun (10.1128/JVI.78.11.6048-
788 6054.2004).
789 40. J. K. Millet, G. R. Whittaker, Host cell entry of Middle East respiratory syndrome coronavirus
790 after two-step, furin-mediated activation of the spike protein. *Proc Natl Acad Sci U S A* **111**,
791 15214-15219 (2014); published online EpubOct (10.1073/pnas.1407087111).
792 41. Y. Yamada, D. X. Liu, Proteolytic activation of the spike protein at a novel RRRR/S motif is
793 implicated in furin-dependent entry, syncytium formation, and infectivity of coronavirus
794 infectious bronchitis virus in cultured cells. *J Virol* **83**, 8744-8758 (2009); published online
795 EpubSep (10.1128/JVI.00613-09).
796 42. Y. W. Kam, Y. Okumura, H. Kido, L. F. Ng, R. Bruzzone, R. Altmeyer, Cleavage of the SARS
797 coronavirus spike glycoprotein by airway proteases enhances virus entry into human
798 bronchial epithelial cells in vitro. *PLoS One* **4**, e7870 (2009); published online EpubNov
799 (10.1371/journal.pone.0007870).
800 43. M. Kawase, K. Shirato, S. Matsuyama, F. Taguchi, Protease-mediated entry via the endosome
801 of human coronavirus 229E. *J Virol* **83**, 712-721 (2009); published online EpubJan
802 (10.1128/JVI.01933-08).

- 803 44. Z. Qiu, S. T. Hingley, G. Simmons, C. Yu, J. Das Sarma, P. Bates, S. R. Weiss, Endosomal
804 proteolysis by cathepsins is necessary for murine coronavirus mouse hepatitis virus type 2
805 spike-mediated entry. *J Virol* **80**, 5768-5776 (2006); published online EpubJun
806 (10.1128/JVI.00442-06).
- 807 45. K. Shirato, M. Kawase, S. Matsuyama, Middle East respiratory syndrome coronavirus
808 infection mediated by the transmembrane serine protease TMPRSS2. *J Virol* **87**, 12552-12561
809 (2013); published online EpubDec (10.1128/JVI.01890-13).
- 810 46. G. Simmons, D. N. Gosalia, A. J. Rennekamp, J. D. Reeves, S. L. Diamond, P. Bates, Inhibitors
811 of cathepsin L prevent severe acute respiratory syndrome coronavirus entry. *Proc Natl Acad
812 Sci U S A* **102**, 11876-11881 (2005); published online EpubAug (10.1073/pnas.0505577102).
- 813 47. S. Bertram, R. Dijkman, M. Habjan, A. Heurich, S. Gierer, I. Glowacka, K. Welsch, M. Winkler,
814 H. Schneider, H. Hofmann-Winkler, V. Thiel, S. Pohlmann, TMPRSS2 activates the human
815 coronavirus 229E for cathepsin-independent host cell entry and is expressed in viral target
816 cells in the respiratory epithelium. *J Virol* **87**, 6150-6160 (2013); published online EpubJun
817 (10.1128/JVI.03372-12).
- 818 48. S. Gierer, S. Bertram, F. Kaup, F. Wrensch, A. Heurich, A. Kramer-Kuhl, K. Welsch, M. Winkler,
819 B. Meyer, C. Drosten, U. Dittmer, T. von Hahn, G. Simmons, H. Hofmann, S. Pohlmann, The
820 spike protein of the emerging betacoronavirus EMC uses a novel coronavirus receptor for
821 entry, can be activated by TMPRSS2, and is targeted by neutralizing antibodies. *J Virol* **87**,
822 5502-5511 (2013); published online EpubMay (10.1128/JVI.00128-13).
- 823 49. I. Glowacka, S. Bertram, M. A. Muller, P. Allen, E. Soilleux, S. Pfefferle, I. Steffen, T. S.
824 Tsegaye, Y. He, K. Gnirss, D. Niemeyer, H. Schneider, C. Drosten, S. Pohlmann, Evidence that
825 TMPRSS2 activates the severe acute respiratory syndrome coronavirus spike protein for
826 membrane fusion and reduces viral control by the humoral immune response. *J Virol* **85**,
827 4122-4134 (2011); published online EpubMay (10.1128/JVI.02232-10).
- 828 50. K. Shirato, S. Matsuyama, M. Ujike, F. Taguchi, Role of proteases in the release of porcine
829 epidemic diarrhea virus from infected cells. *J Virol* **85**, 7872-7880 (2011); published online
830 EpubAug (10.1128/JVI.00464-11).
- 831 51. K. Shirato, M. Kawase, S. Matsuyama, Wild-type human coronaviruses prefer cell-surface
832 TMPRSS2 to endosomal cathepsins for cell entry. *Virology* **517**, 9-15 (2018); published online
833 Epub04 (10.1016/j.virol.2017.11.012).
- 834 52. T. J. Harvey, J. D. Hooper, S. A. Myers, S. A. Stephenson, L. K. Ashworth, J. A. Clements,
835 Tissue-specific expression patterns and fine mapping of the human kallikrein (KLK) locus on
836 proximal 19q13.4. *J Biol Chem* **275**, 37397-37406 (2000); published online EpubDec
837 (10.1074/jbc.M004525200).
- 838 53. J. L. Shaw, E. P. Diamandis, Distribution of 15 human kallikreins in tissues and biological
839 fluids. *Clin Chem* **53**, 1423-1432 (2007); published online EpubAug
840 (10.1373/clinchem.2007.088104).
- 841 54. N. Emami, E. P. Diamandis, New insights into the functional mechanisms and clinical
842 applications of the kallikrein-related peptidase family. *Mol Oncol* **1**, 269-287 (2007);
843 published online EpubDec (10.1016/j.molonc.2007.09.003).
- 844 55. J. Clements, J. Hooper, Y. Dong, T. Harvey, The expanded human kallikrein (KLK) gene family:
845 genomic organisation, tissue-specific expression and potential functions. *Biol Chem* **382**, 5-14
846 (2001); published online EpubJan (10.1515/BC.2001.002).
- 847 56. M. Kalinska, U. Meyer-Hoffert, T. Kantyka, J. Potempa, Kallikreins - The melting pot of activity
848 and function. *Biochimie* **122**, 270-282 (2016); published online EpubMar
849 (10.1016/j.biochi.2015.09.023).
- 850 57. N. Memari, L. Grass, T. Nakamura, I. Karakucuk, E. P. Diamandis, Human tissue kallikrein 9:
851 production of recombinant proteins and specific antibodies. *Biol Chem* **387**, 733-740 (2006);
852 published online EpubJun (10.1515/BC.2006.092).

- 853 58. N. Memari, W. Jiang, E. P. Diamandis, L. Y. Luo, Enzymatic properties of human kallikrein-
854 related peptidase 12 (KLK12). *Biol Chem* **388**, 427-435 (2007); published online EpubApr
855 (10.1515/BC.2007.049).
- 856 59. M. R. Darling, L. Jackson-Boeters, T. D. Daley, E. P. Diamandis, Human kallikrein 13 expression
857 in salivary gland tumors. *Int J Biol Markers* **21**, 106-110 (2006); published online Epub2006
858 Apr-Jun (
- 859 60. G. Sotiropoulou, G. Pampalakis, E. P. Diamandis, Functional roles of human kallikrein-related
860 peptidases. *J Biol Chem* **284**, 32989-32994 (2009); published online EpubNov
861 (10.1074/jbc.R109.027946).
- 862 61. N. Gruba, E. Bielecka, M. Wysocka, A. Wojtysiak, M. Brzezińska-Bodał, K. Sychowska, M.
863 Kalińska, M. Magoch, A. Pęczak, K. Falkowski, M. Wiśniewska, L. Szaśiadek, K. Płaza, E. Kroll, A.
864 Pejkovska, M. Rehders, K. Brix, G. Dubin, T. Kantyka, J. Potempa, A. Lesner, Development of
865 Chemical Tools to Monitor Human Kallikrein 13 (KLK13) Activity. *Int J Mol Sci* **20**, (2019);
866 published online EpubMar (10.3390/ijms20071557).
- 867 62. U. Meyer-Hoffert, Z. Wu, T. Kantyka, J. Fischer, T. Latendorf, B. Hansmann, J. Bartels, Y. He, R.
868 Gläser, J. M. Schröder, Isolation of SPINK6 in human skin: selective inhibitor of kallikrein-
869 related peptidases. *J Biol Chem* **285**, 32174-32181 (2010); published online EpubOct
870 (10.1074/jbc.M109.091850).
- 871 63. T. Kantyka, J. Fischer, Z. Wu, W. Declercq, K. Reiss, J. M. Schröder, U. Meyer-Hoffert,
872 Inhibition of kallikrein-related peptidases by the serine protease inhibitor of Kazal-type 6.
873 *Peptides* **32**, 1187-1192 (2011); published online EpubJun (10.1016/j.peptides.2011.03.009).
- 874 64. C. Liu, Y. Ma, Y. Yang, Y. Zheng, J. Shang, Y. Zhou, S. Jiang, L. Du, J. Li, F. Li, Cell Entry of
875 Porcine Epidemic Diarrhea Coronavirus Is Activated by Lysosomal Proteases. *J Biol Chem* **291**,
876 24779-24786 (2016); published online EpubNov 18 (10.1074/jbc.M116.740746).
- 877 65. X. Ou, H. Guan, B. Qin, Z. Mu, J. A. Wojdyla, M. Wang, S. R. Dominguez, Z. Qian, S. Cui, Crystal
878 structure of the receptor binding domain of the spike glycoprotein of human betacoronavirus
879 HKU1. *Nat Commun* **8**, 15216 (2017); published online EpubMay (10.1038/ncomms15216).
- 880 66. I. E. Ekholm, M. Brattsand, T. Egelrud, Stratum corneum tryptic enzyme in normal epidermis:
881 a missing link in the desquamation process? *J Invest Dermatol* **114**, 56-63 (2000); published
882 online EpubJan (10.1046/j.1523-1747.2000.00820.x).
- 883 67. A. Lundström, T. Egelrud, Stratum corneum chymotryptic enzyme: a proteinase which may
884 be generally present in the stratum corneum and with a possible involvement in
885 desquamation. *Acta Derm Venereol* **71**, 471-474 (1991).
- 886 68. J. D. Bartlett, Dental enamel development: proteinases and their enamel matrix substrates.
887 *ISRN Dent* **2013**, 684607 (2013); published online EpubSep (10.1155/2013/684607).
- 888 69. A. Cho, N. Haruyama, B. Hall, M. J. Danton, L. Zhang, P. Arany, D. J. Mooney, Y. Harichane, M.
889 Goldberg, C. W. Gibson, A. B. Kulkarni, TGF- β regulates enamel mineralization and
890 maturation through KLK4 expression. *PLoS One* **8**, e82267
891 (2013)10.1371/journal.pone.0082267).
- 892 70. P. S. Hart, T. C. Hart, M. D. Michalec, O. H. Ryu, D. Simmons, S. Hong, J. T. Wright, Mutation in
893 kallikrein 4 causes autosomal recessive hypomaturation amelogenesis imperfecta. *J Med*
894 *Genet* **41**, 545-549 (2004); published online EpubJul (
- 895 71. P. Papagerakis, G. Pannone, L. I. Zheng, M. Athanassiou-Papaefthymiou, Y. Yamakoshi, H. S.
896 McGuff, O. Shkeir, K. Ghirtis, S. Papagerakis, Clinical significance of kallikrein-related
897 peptidase-4 in oral cancer. *Anticancer Res* **35**, 1861-1866 (2015); published online EpubApr (
- 898 72. X. Charest-Morin, A. Raghavan, M. L. Charles, T. Kolodka, J. Bouthillier, M. Jean, M. S.
899 Robbins, F. Marceau, Pharmacological effects of recombinant human tissue kallikrein on
900 bradykinin B2 receptors. *Pharmacol Res Perspect* **3**, e00119 (2015); published online
901 EpubMar (10.1002/prp2.119).
- 902 73. Y. Wang, W. Luo, G. Reiser, Trypsin and trypsin-like proteases in the brain: proteolysis and
903 cellular functions. *Cell Mol Life Sci* **65**, 237-252 (2008); published online EpubJan
904 (10.1007/s00018-007-7288-3).

- 905 74. K. Ogawa, T. Yamada, Y. Tsujioka, J. Taguchi, M. Takahashi, Y. Tsuboi, Y. Fujino, M. Nakajima,
906 T. Yamamoto, H. Akatsu, S. Mitsui, N. Yamaguchi, Localization of a novel type trypsin-like
907 serine protease, neurosin, in brain tissues of Alzheimer's disease and Parkinson's disease.
908 *Psychiatry Clin Neurosci* **54**, 419-426 (2000); published online EpubAug (10.1046/j.1440-
909 1819.2000.00731.x).
- 910 75. J. Lou, H. Si, Y. Chen, X. Sun, H. Zhang, A. Niu, C. Hu, Correlation between KLK6 expression
911 and the clinicopathological features of glioma. *Contemp Oncol (Pozn)* **18**, 246-251
912 (2014)10.5114/wo.2014.44628).
- 913 76. C. Cerqueira, P. Samperio Ventayol, C. Vogeley, M. Schelhaas, Kallikrein-8 Proteolytically
914 Processes Human Papillomaviruses in the Extracellular Space To Facilitate Entry into Host
915 Cells. *J Virol* **89**, 7038-7052 (2015); published online EpubJul (10.1128/JVI.00234-15).
- 916 77. B. S. Hamilton, G. R. Whittaker, Cleavage activation of human-adapted influenza virus
917 subtypes by kallikrein-related peptidases 5 and 12. *J Biol Chem* **288**, 17399-17407 (2013);
918 published online EpubJun (10.1074/jbc.M112.440362).
- 919 78. M. Magnen, F. Gueugnon, A. Guillon, T. Baranek, V. C. Thibault, A. Petit-Courty, S. J. de Veer,
920 J. Harris, A. A. Humbles, M. Si-Tahar, Y. Courty, Kallikrein-Related Peptidase 5 Contributes to
921 H3N2 Influenza Virus Infection in Human Lungs. *J Virol* **91**, (2017); published online EpubAug
922 (10.1128/JVI.00421-17).
- 923 79. J. Gibo, T. Ito, K. Kawabe, T. Hisano, M. Inoue, N. Fujimori, T. Oono, Y. Arita, H. Nawata,
924 Camostat mesilate attenuates pancreatic fibrosis via inhibition of monocytes and pancreatic
925 stellate cells activity. *Lab Invest* **85**, 75-89 (2005); published online EpubJan
926 (10.1038/labinvest.3700203).
- 927 80. Y. Zhou, P. Vedantham, K. Lu, J. Agudelo, R. Carrion, J. W. Nunneley, D. Barnard, S. Pöhlmann,
928 J. H. McKerrow, A. R. Renslo, G. Simmons, Protease inhibitors targeting coronavirus and
929 filovirus entry. *Antiviral Res* **116**, 76-84 (2015); published online EpubApr
930 (10.1016/j.antiviral.2015.01.011).
- 931 81. S. Matsuyama, K. Shirato, M. Kawase, Y. Terada, K. Kawachi, S. Fukushi, W. Kamitani, Middle
932 East respiratory syndrome coronavirus spike protein is not activated directly by cellular furin
933 during viral entry into target cells. *J Virol*, (2018); published online EpubJul
934 (10.1128/JVI.00683-18).
- 935 82. L. R. de Souza, P. M. Melo, T. Paschoalin, A. K. Carmona, M. Kondo, I. Y. Hirata, M. Blaber, I.
936 Tersariol, J. Takatsuka, M. A. Juliano, L. Juliano, R. A. Gomes, L. Puzer, Human tissue
937 kallikreins 3 and 5 can act as plasminogen activator releasing active plasmin. *Biochem*
938 *Biophys Res Commun* **433**, 333-337 (2013); published online EpubApr
939 (10.1016/j.bbrc.2013.03.001).
- 940 83. D. Andrade, D. M. Assis, J. A. Santos, F. M. Alves, I. Y. Hirata, M. S. Araujo, S. I. Blaber, M.
941 Blaber, M. A. Juliano, L. Juliano, Substrate specificity of kallikrein-related peptidase 13
942 activated by salts or glycosaminoglycans and a search for natural substrate candidates.
943 *Biochimie* **93**, 1701-1709 (2011); published online EpubOct (10.1016/j.biochi.2011.05.037).
- 944 84. M. G. Lawrence, J. Lai, J. A. Clements, Kallikreins on steroids: structure, function, and
945 hormonal regulation of prostate-specific antigen and the extended kallikrein locus. *Endocr*
946 *Rev* **31**, 407-446 (2010); published online EpubAug (10.1210/er.2009-0034).
- 947 85. A. Magklara, L. Grass, E. P. Diamandis, Differential steroid hormone regulation of human
948 glandular kallikrein (hK2) and prostate-specific antigen (PSA) in breast cancer cell lines.
949 *Breast Cancer Res Treat* **59**, 263-270 (2000); published online EpubFeb (
- 950 86. S. Morizane, K. Yamasaki, F. D. Kabigting, R. L. Gallo, Kallikrein expression and cathelicidin
951 processing are independently controlled in keratinocytes by calcium, vitamin D(3), and
952 retinoic acid. *J Invest Dermatol* **130**, 1297-1306 (2010); published online EpubMay
953 (10.1038/jid.2009.435).
- 954 87. K. Oikonomopoulou, K. K. Hansen, M. Saifeddine, N. Vergnolle, I. Tea, M. Blaber, S. I. Blaber,
955 I. Scarisbrick, E. P. Diamandis, M. D. Hollenberg, Kallikrein-mediated cell signalling: targeting

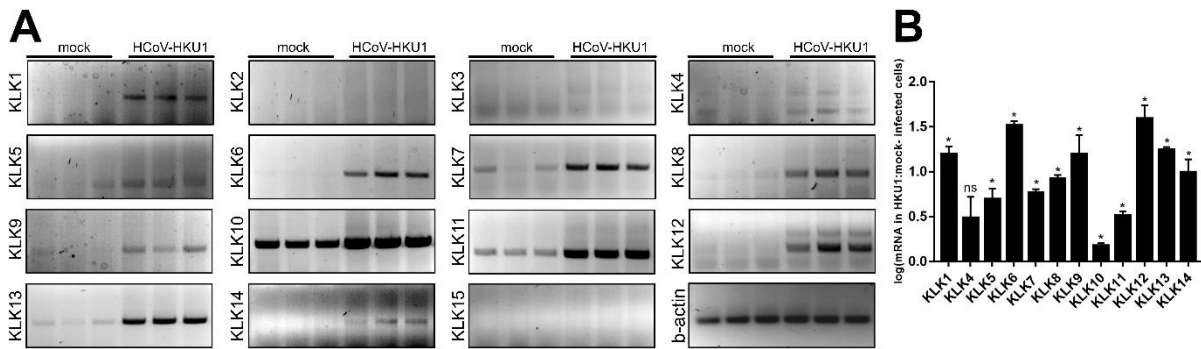
- 956 proteinase-activated receptors (PARs). *Biol Chem* **387**, 817-824 (2006); published online
957 EpubJun (10.1515/BC.2006.104).
- 958 88. M. D. Hollenberg, K. Oikonomopoulou, K. K. Hansen, M. Saifeddine, R. Ramachandran, E. P.
959 Diamandis, Kallikreins and proteinase-mediated signaling: proteinase-activated receptors
960 (PARs) and the pathophysiology of inflammatory diseases and cancer. *Biol Chem* **389**, 643-
961 651 (2008); published online EpubJun (10.1515/BC.2008.077).
- 962 89. K. Oikonomopoulou, K. K. Hansen, M. Saifeddine, I. Tea, M. Blaber, S. I. Blaber, I. Scarisbrick,
963 P. Andrade-Gordon, G. S. Cottrell, N. W. Bunnett, E. P. Diamandis, M. D. Hollenberg,
964 Proteinase-activated receptors, targets for kallikrein signaling. *J Biol Chem* **281**, 32095-32112
965 (2006); published online EpubOct (10.1074/jbc.M513138200).
- 966 90. A. Seliga, M. H. Lee, N. C. Fernandes, V. Zuluaga-Ramirez, M. Didukh, Y. Persidsky, R. Potula,
967 S. Gallucci, U. Sriram, Kallikrein-Kinin System Suppresses Type I Interferon Responses: A
968 Novel Pathway of Interferon Regulation. *Front Immunol* **9**, 156
969 (2018)10.3389/fimmu.2018.00156).
- 970 91. C. D. Petraki, P. A. Papanastasiou, V. N. Karavana, E. P. Diamandis, Cellular distribution of
971 human tissue kallikreins: immunohistochemical localization. *Biol Chem* **387**, 653-663 (2006);
972 published online EpubJun (10.1515/BC.2006.084).
- 973 92. T. Heald-Sargent, T. Gallagher, Ready, set, fuse! The coronavirus spike protein and acquisition
974 of fusion competence. *Viruses* **4**, 557-580 (2012); published online Epub04
975 (10.3390/v4040557).
- 976 93. J. T. Earnest, M. P. Hantak, K. Li, P. B. McCray, S. Perlman, T. Gallagher, The tetraspanin CD9
977 facilitates MERS-coronavirus entry by scaffolding host cell receptors and proteases. *PLoS*
978 *Pathog* **13**, e1006546 (2017); published online EpubJul (10.1371/journal.ppat.1006546).
- 979 94. J. Moffat, D. A. Grueneberg, X. Yang, S. Y. Kim, A. M. Kloepper, G. Hinkle, B. Piqani, T. M.
980 Eisenhaure, B. Luo, J. K. Grenier, A. E. Carpenter, S. Y. Foo, S. A. Stewart, B. R. Stockwell, N.
981 Hacohen, W. C. Hahn, E. S. Lander, D. M. Sabatini, D. E. Root, A lentiviral RNAi library for
982 human and mouse genes applied to an arrayed viral high-content screen. *Cell* **124**, 1283-1298
983 (2006); published online EpubMar (10.1016/j.cell.2006.01.040).
- 984 95. A. Horani, A. Nath, M. G. Wasserman, T. Huang, S. L. Brody, Rho-associated protein kinase
985 inhibition enhances airway epithelial Basal-cell proliferation and lentivirus transduction. *Am J*
986 *Respir Cell Mol Biol* **49**, 341-347 (2013); published online EpubSep (10.1165/rcmb.2013-
987 0046TE).
- 988 96. A. Milewska, J. Ciejka, K. Kaminski, A. Karewicz, D. Bielska, S. Zeglen, W. Karolak, M.
989 Nowakowska, J. Potempa, B. J. Bosch, K. Pyrc, K. Szczubialka, Novel polymeric inhibitors of
990 HCoV-NL63. *Antiviral research* **97**, 112-121 (2013); published online EpubFeb
991 (10.1016/j.antiviral.2012.11.006).
- 992 97. J. R. Kovalski, A. Bhaduri, A. M. Zehnder, P. H. Neela, Y. Che, G. G. Wozniak, P. A. Khavari, The
993 Functional Proximal Proteome of Oncogenic Ras Includes mTORC2. *Mol Cell* **73**, 830-
994 844.e812 (2019); published online Epub02 (10.1016/j.molcel.2018.12.001).
- 995 98. A. Milewska, K. Kaminski, J. Ciejka, K. Kosowicz, S. Zeglen, J. Wojarski, M. Nowakowska, K.
996 Szczubialka, K. Pyrc, HTCC: Broad Range Inhibitor of Coronavirus Entry. *PLoS One* **11**,
997 e0156552 (2016)10.1371/journal.pone.0156552).
- 998 99. A. J. Lizama, Y. Andrade, P. Colivoro, J. Sarmiento, C. E. Matus, C. B. Gonzalez, K. D. Bhoola, P.
999 Ehrenfeld, C. D. Figueroa, Expression and bioregulation of the kallikrein-related peptidases
1000 family in the human neutrophil. *Innate Immun* **21**, 575-586 (2015); published online EpubAug
1001 (10.1177/1753425914566083).

1002

1003 **FIGURE TITLES AND LEGENDS**

1004 **FIGURE 1.**

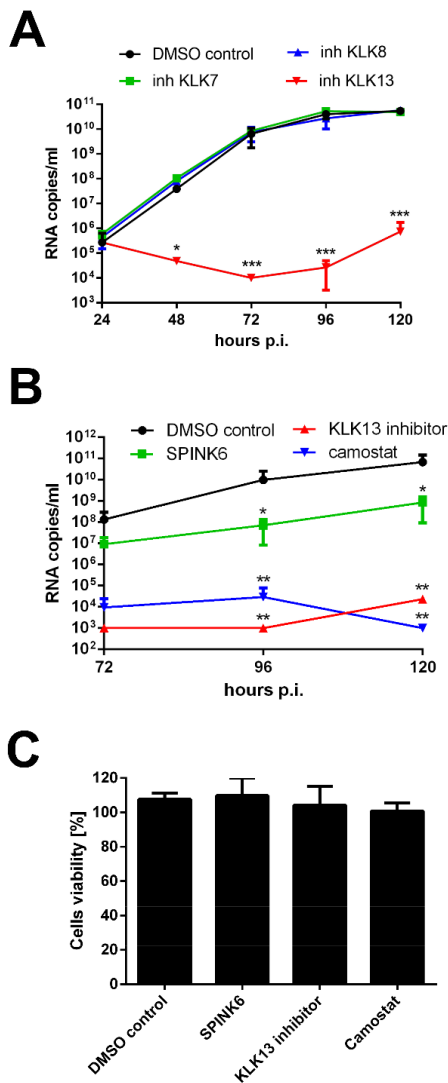
1005



1006

1007 **Figure 1. Up-regulation of several KLKs after HCoV-HKU1 infection in HAE.**
1008 HAE cultures were infected with HCoV-HKU1 (10^6 RNA copies per ml) or mock for 2 h at
1009 32°C and cultured for 5 days. Cellular RNA was isolated, treated with DNase, reverse
1010 transcribed and each KLKs mRNA was amplified using specific primers. The analysis was
1011 performed two times using cells obtained from different donors, each time in triplicate. (A)
1012 Amplified PCR products were resolved and detected in 1.5% (w:v) agarose gel in $1 \times$ TAE
1013 buffer. (B) The expression of each KLK comparing to β -actin control was assessed semi-
1014 quantitatively by densitometry and is presented as a log change of signal specific for KLKs
1015 mRNA in HCoV-HKU1-infected cells, compared to the mock-infected cells. The experiment
1016 was performed three times using cells from different donors, each time with three biological
1017 replicates. For comparisons by Student's t-test, *Indicates $P < 0.05$; ns, not significant.

1018 **FIGURE 2.**

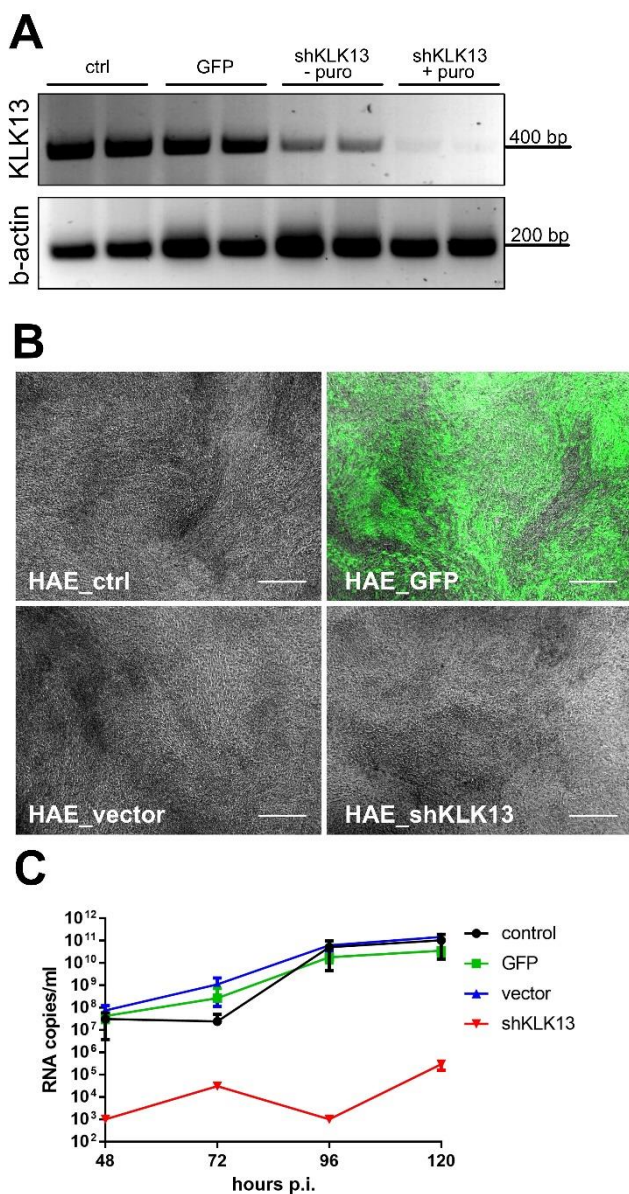


1019

1020 **Figure 2. HCoV-HKU1 infection is dependent on KLK13 activity.**

1021 HAE cultures were inoculated with HCoV-HKU1 (10^6 RNA copies per ml) for 2 h at 32°C in
1022 the presence of 10 μ M KLKs inhibitors (**Table 1**) or DMSO (**A**); 10 μ g/ml SPINK6, 10 μ M
1023 KLK13 inhibitor, 100 μ M camostat or DMSO (**B**). To analyze virus replication kinetics, each
1024 day post-infection, 100 μ l of 1 \times PBS with a given inhibitor was applied to the apical surface
1025 of HAE cultures and collected after 10 min incubation at 32°C. Replication of HCoV-HKU1
1026 was evaluated using an RT-qPCR and the data are presented as RNA copy number per ml. The
1027 assay was performed twice, each time in triplicate, and average values with standard errors are
1028 presented. Statistical significance was assessed with the Student's t-test, and the asterisks
1029 indicate: * $P < 0.05$, ** $P < 0.005$, *** $P < 0.0005$. (**C**) Cytotoxicity of inhibitors in HAE
1030 cultures. Cell viability was assessed with the XTT assay on mock-treated cells at 120 h post-
1031 infection. Data on the y-axis represent the percentage values obtained for the untreated
1032 reference samples. The assay was performed in triplicate and average values with standard
1033 errors are presented.

1034 **FIGURE 3.**

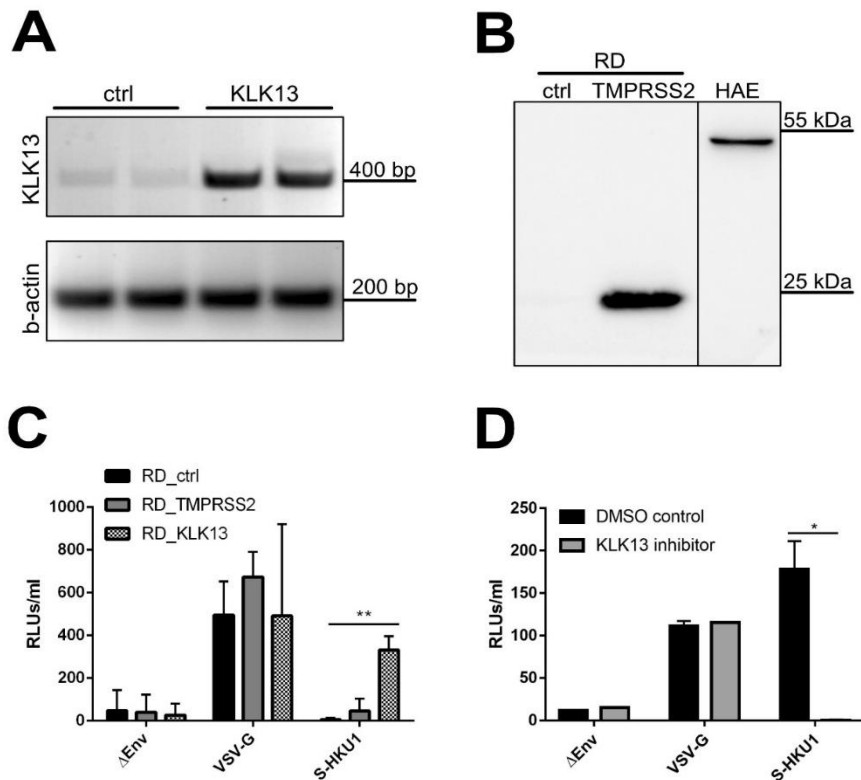


1035

1036 **Figure 3. HCoV-HKU1 does not replicate in HAE cells deficient in KLK13.**

1037 Primary human epithelial cells were transduced with lentiviral vectors harboring the GFP
1038 (HAE_GFP) protein, empty pLKO.1-TRC vector (HAE_vector) or shRNA for KLK13 mRNA
1039 (HAE_shKLK13). As a control, not transduced HAE cultures were used (HAE_ctrl). (A) The
1040 KLK13 mRNA was evaluated before (- puro) and after puromycin (+ puro) selection of
1041 positively transduced cells, β -actin was used as an internal control. (B) Microscopic
1042 examination of all HAE cultures after 4 weeks culture in ALI at 37°C. Scale bar = 200 μ m. (C)
1043 All HAE cultures were inoculated with HCoV-HKU1 (10^6 RNA copies per ml) for 2 h at 32°C
1044 and cultured for 5 days. Each day post-infection, 100 μ l of 1 \times PBS was applied to the apical
1045 surface of HAE cultures and collected after 10 min incubation at 32°C. Replication of HCoV-
1046 HKU1 was evaluated using an RT-qPCR and the data are presented as RNA copy number per
1047 ml. The assay was performed twice, each time in triplicate, and average values with standard
1048 errors are presented.

1049 **FIGURE 4.**

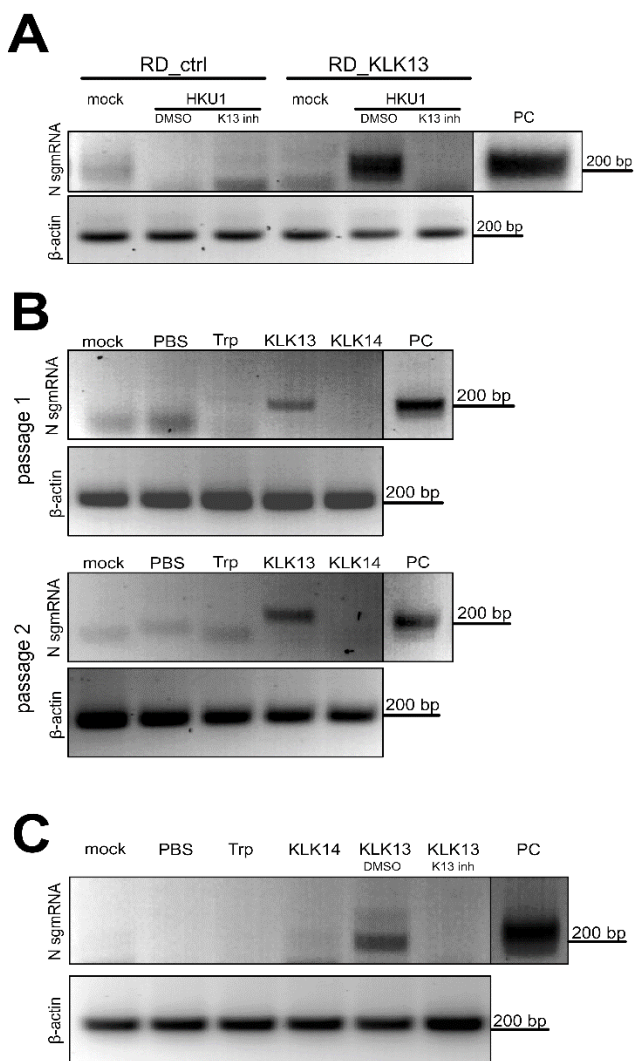


1050

1051 **Figure 4. RD cells expressing KLK13 are permissive for the HCoV-HKU1**
 1052 **pseudoviruses.**

1053 (A) RD cells were transduced with lentiviral vectors harboring the KLK13 gene (KLK13) or
 1054 empty vector (ctrl). The presence of KLK13 mRNA was evaluated in RD cells after blasticidin
 1055 selection; β-actin was used as an internal control. (B) RD cells were transduced with lentiviral
 1056 vectors harboring the TMPRSS2 gene (TMPRSS2) or empty vector (ctrl). After blasticidin
 1057 selection, cells were lysed and proteins were analyzed with SDS-PAGE. TMPRSS2 was
 1058 detected in RD cell lysates (50 μg of protein per lane) and HAE cultures lysate (25 μg of protein
 1059 per lane) using the specific antibody. (C) RD control (RD_ctrl), TMPRSS2-expressing
 1060 (RD_TMPRSS2) or KLK13-expressing (RD_KLK13) cells were transduced with HIV
 1061 pseudoviruses decorated with VSV-G protein (VSV-G), S-HKU1 glycoprotein (S-HKU1) or
 1062 control viruses without the fusion protein (ΔEnv). After 72 h at 37°C, the entry of pseudoviruses
 1063 was measured by means of luminescence signal in cell lysates. The assay was performed twice,
 1064 each time in triplicate, and average values with standard errors are presented. For comparisons
 1065 by Student's t-test, **Indicates P < 0.005. (D) HAE cultures were inoculated with HIV
 1066 pseudoviruses harboring VSV-G control protein, S-HKU1 or control viruses without the fusion
 1067 protein (ΔEnv) in the presence of KLK13 inhibitor (10 μM) or DMSO. After 72 h at 37°C the
 1068 entry of pseudoviruses was measured by means of luminescence signal in cell lysates (RLUs
 1069 per ml of lysate sample). The assay was performed in duplicate, and average values with
 1070 standard errors are presented. Statistical significance was assessed with the Student's t-test, and
 1071 the asterisk indicates P < 0.05.

1072 **FIGURE 5.**



1073
1074 **Figure 5. HCoV-HKU1 replicates in RD cells expressing KLK13 protease.**
1075 (A) Control (RD_ctrl) or KLK13-expressing (RD_KLK13) cells were inoculated with HCoV-
1076 HKU1 (10^6 RNA copies per ml) or mock in the presence of 10 μ M KLK 13 inhibitor (K13 inh)
1077 or control DMSO. After 7 days culture at 32°C, total RNA was isolated, reverse transcribed and
1078 subgenomic mRNA for N protein was detected in semi-nested PCR, β -actin was used as an
1079 internal control. PC = positive control from virus-infected HAE cells. (B) HCoV-HKU1 was
1080 incubated with 200 nM trypsin (Trp), KLK13, KLK14 or PBS for 2 h at 32°C and further
1081 applied on the RD cells. After 7 days at 32°C total RNA was isolated, reverse transcribed and
1082 subgenomic mRNA for N protein was detected in semi-nested PCR (passage 1).
1083 Simultaneously, 1 ml of cell culture supernatant was harvested and applied to freshly seeded
1084 RD cells with medium supplemented with fresh enzymes. After 7 days at 32°C, subgenomic
1085 mRNA for the N protein was detected in semi-nested PCR (passage 2). β -actin was used as an
1086 internal control. (C) HCoV-HKU1 was incubated with 200 nM trypsin (Trp), KLK14, KLK13
1087 with KLK13 inhibitor (K13 inh), control DMSO (DMSO), or PBS for 2 h at 32°C and further
1088 applied onto the RD cells. Subgenomic mRNA for N protein was detected in semi-nested PCR;
1089 β -actin was used as an internal control. PC: positive control from virus-infected HAE cultures.

